Trends in Analytical Chemistry 97 (2017) 428–444

Contents lists available at ScienceDirect

Trends in Analytical Chemistry

journal homepage: www.elsevier.com/locate/trac

Helicobacter pylori point-of-care diagnosis: Nano-scale biosensors and microfluidic systems

Rahim Nosrati [a, b], Behrouz Golichenari [a, c], Alireza Nezami [b], Seyed Mohammad Taghdisi [d], Bahareh Karimi [e], Mohammad Ramezani [f], Khalil Abnous [b, *], Seyed Ali Mousavi Shaegh [g, h, **]

[a] Student Research Committee, Department of Pharmaceutical Biotechnology, School of Pharmacy, Mashhad University of Medical Sciences, Mashhad, Iran
[b] Pharmaceutical Research Center, Mashhad University of Medical Sciences, Mashhad, Iran
[c] Biotechnology Research Center, Mashhad University of Medical Sciences, Mashhad, Iran
[d] Targeted Drug Delivery Research Center, Mashhad University of Medical Sciences, Mashhad, Iran
[e] Department of Microbiology, Lahijan branch, Islamic Azad University, Lahijan, Iran
[f] Nanotechnology Research Center, Mashhad University of Medical Sciences, Mashhad, Iran
[g] Orthopedic Research Center, School of Medicine, Mashhad University of Medical Sciences, Mashhad, Iran
[h] Clinical Research Unit, Mashhad University of Medical Sciences, Mashhad, Iran

ARTICLE INFO

Article history:
Available online 21 October 2017

Keywords:
H. pylori
Biosensors
Nanosensors
Lateral flow assay
Microfluidics
Point-of-care (POC) detection
Paper-based diagnostics

ABSTRACT

Helicobacter pylori is a species of bacteria that can colonize the human stomach mucosa. It is closely associated with gastric diseases. The restrictions of traditional methods have encouraged the development of innovative methods for rapid, reliable, and cost-effective diagnosis of *H. pylori* infection. In recent years, the concept of biosensor and microfluidic-based devices has opened new horizons in high-precision detection. Once combined with nanomaterials, nano-scale biosensors and microfluidic systems provide powerful analytical platforms for point of care (POC) diagnosing of *H. pylori*. In this article, a brief overview of general aspects of *H. pylori* infection and current diagnostic methods are firstly discussed. In addition, a clear and concise review of recent advances of biosensors, paper-based and microfluidic systems based on nanomaterials for the detection of *H. pylori* are discussed herein. Subsequently, the latest development of integrated and miniaturized microfluidic biosensing technologies for POC detection of *H. pylori* is explained.

1. Introduction

Helicobacter pylori (*H. pylori*) infection is caused by a spiral-shaped, gram-negative bacterium colonized the apical surface of human stomach epithelial cells [1,2]. *H. pylori* infection is one of the most frequent and persistent bacterial infections in many countries because of its widespread prevalence [3]. *H. pylori* is involved in various gastric pathologies such as peptic, duodenal and gastric ulcers [4], gastric cancer [5,6], chronic atrophic gastritis [7], mucosa-associated lymphoid tissue lymphoma (MALT) [8] and liver cancer [9]. *H. pylori* infection may damage the tissue by an amalgam of host, environmental, and different types of bacterial virulence factors [10,11]. Several virulence-factors of *H. pylori* have been reported to play a major role in the pathogenesis of *H. pylori* especially the urease enzymes, CagA (cytotoxin-associated gene A), VacA (vacuolating cytotoxin gene A), and outer membrane proteins [12,13]. The more detailed mechanism of pathogen-host interplay in the pathogenesis of *H. pylori* infection is as follows:

H. pylori with several virulence factors interact with gastric epithelial cells through an interaction between bacterial adhesins and the host-cell receptors [1,13]. Following attachment to the cell, bacteria produce the urease enzyme, which hydrolyses urea into NH_3 and CO_2 (Fig. 1A). Ammonium ions neutralize the gastric acid and the bacteria colonize in the gastric mucosa and release secretory enzymes such as mucinase, protease, and phospholipase lead to gastric mucosal injury [14]. Subsequently, increase in gastric acid levels result alteration in gastric normal cell through the

* Corresponding author.
** Corresponding author. Orthopedic Research Center, School of Medicine, Mashhad University of Medical Sciences, Mashhad, Iran.
E-mail addresses: Abnouskh@mums.ac.ir (K. Abnous), Mousavisha@mums.ac.ir (S.A.M. Shaegh).

https://doi.org/10.1016/j.trac.2017.10.013
0165-9936/

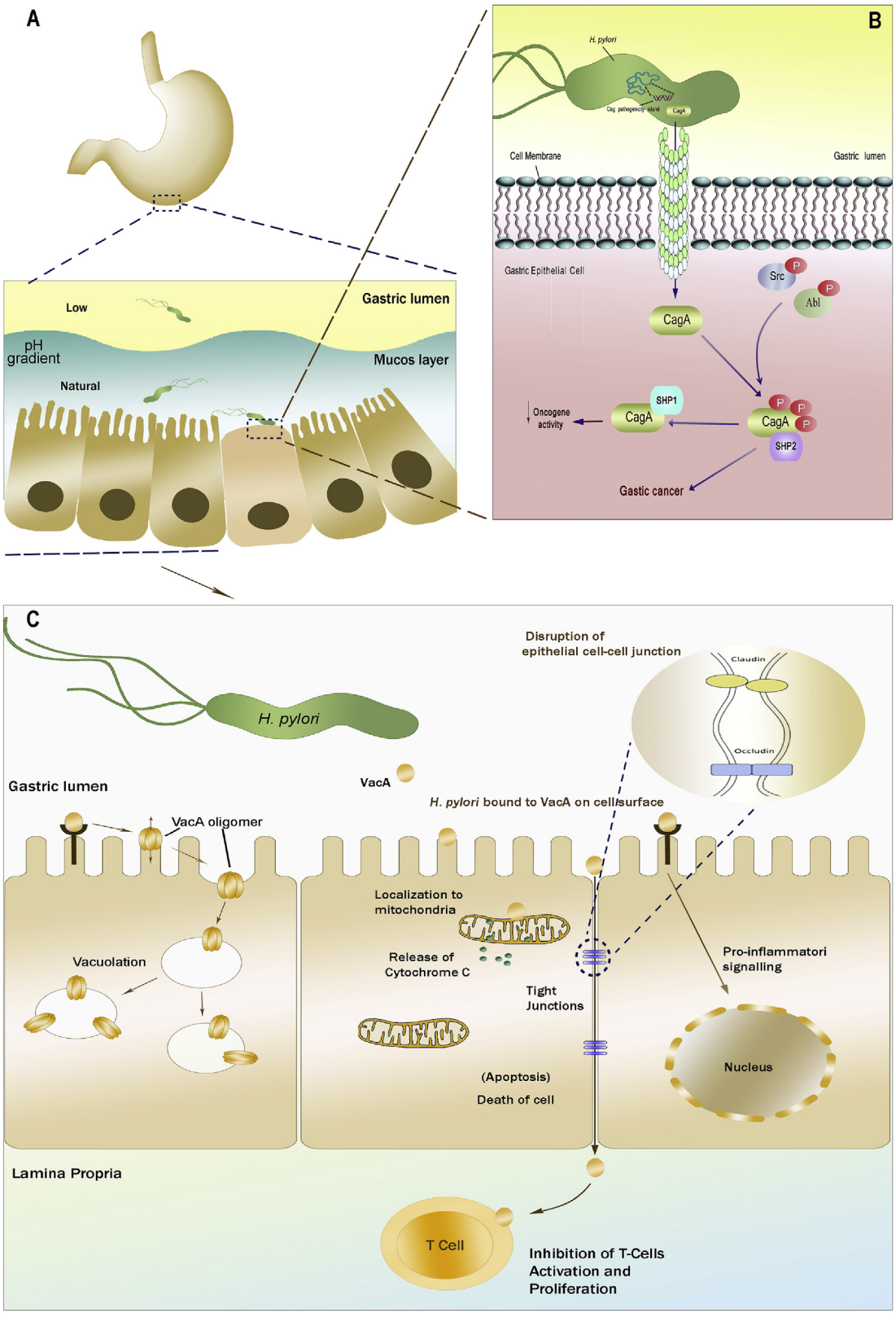

Fig. 1. An overview of *Helicobacter pylori* virulence factors and pathogenesis. (A) Colonization and interaction between bacterial adhesin and the host-cell receptor, (B) Induction of cytotoxin-associated gene A (CagA) gene as a mechanism of cellular and DNA regulatory inhibition, (C) VacA (vacuolating cytotoxin gene A) injection and variety of effects on target cells. Reproduce from published papers [11,18,19].

introduction of the CagA protein and peptidoglycan of Helicobacter [15]. The CagA protein which is encoded by the cag pathogenicity island (PAI) is injected into the host cell through the type IV secretion system (T4SS) [16]. The translocated CagA protein localizes to the inner leaflet of the cell membrane and is functionally activated by sequentially phosphorylation of its EPIYA motifs by host kinases c-Src and c-Abl. Phosphorylated CagA interacts with intracellular signal transducers, deregulates their activities and increases the risk of gastric carcinoma [17] (Fig. 1B).

Vacuolating cytotoxin gene A is the second most potent virulence factor that is produced during *H. pylori* infection [18]. The VacA protein is released outside of the *H. pylori* where it binds to the outer surface of a stomach cell which consequently leads to epithelial cell vacuolation [19]. VacA can exert a variety of other effects on target cells, including membrane-channel formation, inhibition of T-cell activation and proliferation and binding to cell-membrane receptors followed by initiation of a pro-inflammatory signaling [20,21]. The VacA protein also localizes to the mitochondrial membrane and induces release of cytochrome *c* from mitochondria leading to the activation of an apoptotic cascade. This cellular destruction sends signals to the immune system by the production of cytokines, leading to tissue infiltration of immune cells [19,22]. Lastly, release of free radicals from the granulocytes causes the damage. Autoantibodies, induced by *Helicobacter*, kill acid secreting parietal cells, eventually leading to gastric-related disease [15] (Fig. 1C).

A number of tests with varying precision and sensitivity have been developed to identify *H. pylori* infection. Diagnostic methods for *H. pylori* infection have generally been categorized into direct (invasive) and indirect (noninvasive) tests [23]. The invasive methods such as rapid urease test (RUT), polymerase chain reaction (PCR), histology and culture are based on direct identifying the microorganism by upper gastrointestinal endoscopy and gastric biopsies [23–25]. Noninvasive tests can be employed for initial diagnosis of *H. pylori* infection which can be performed on serum [26], saliva [27], stool [28], or breath samples [29]. Serology (detection of antibodies against *H. pylori)*, ^{13}C-urea breath test (^{13}C-UBT), stool antigen test (SAT) (or fecal antigen test (FAT)), and *H. pylori* saliva antigen test (HPS) can be performed at non-invasive procedures [30,31]. In addition, PCR-based detection could be categorized under noninvasive methods [32]. Invasive tests can be used for monitoring the extent of injury in the stomach and direct identification of the *H. pylori* organism, while indirect tests can be only used to identify *H. pylori* in a sample [30]. The selection of an appropriate diagnostic test depends on various parameters, including the sensitivity, specificity, cost, accessibility, reliability, limitations of the test, clinical setting, prevalence of infection in the population, and pretest probability of infection [32]. In general, the conventional methods have some restrictions since they necessitate incorporation of expensive equipment and utilize high quantity of costly reagents [33].

The major challenge of treating illnesses associated with *H. pylori* infection is rapid diagnosis and treatment of virulent in the early stages [15]. Indeed, many methods have been developed as rapid diagnostic testing (RDT) [32] and point of-care (POC) diagnostics [34] for *H. pylori* infection. Nano-scale biosensors and microfluidic systems provide powerful analytical platforms for RDT and POC diagnosis of *H. pylori*. These methods enable performing rapid analysis and provide results within a couple of minutes to a few hours [35]. With remarkable achievements in nanoscience, nanomaterials have opened new options for designing biosensors and immunosensors and display great potential for monitoring biomolecules and sensitive detection of target analytes in biosensing platforms [36]. The microfluidic-based systems and lab-on-a-chip (LOC) devices offer significant advantages including high throughput and speed, portability, low cost, and automation for use in POC diagnostics [37–39].

In this paper, a clear and concise review of recent advances associated with rapid and quantitative detection of *H. pylori* using of nanomaterial-based biosensors and microfluidic systems was discussed. Subsequently, the latest development of integrated microfluidic biosensing technologies for POC detection of *H. pylori* was explained.

2. Nano-biosensors for analysis of *H. pylori*

Function of *H. pylori* rapid diagnostic approaches can be mainly classified into four categories as (i) detection of *H. pylori* specific antigens; (ii) molecular recognition of the specific *H. pylori* nucleic acid sequences; (iii) quick biochemical reaction tests, and (iv) serologic revealing of *H. pylori* specific antibodies [32]. For rapid diagnosis of *H. pylori*, biosensors can play critical roles [34]. In general, a biosensor is a compact analytical device, which is capable of providing selective quantitative or semi-quantitative analytical information using by combining a biological recognition element with a signal conversion unit (a transducer) [40,41]. Nowadays, biosensors coupled with nanomaterials provide a hybrid nano-biosensor with synergetic properties and functions. The unique chemical and physical properties of nanomaterials (NMs) and especially nanoparticles (NPs) make them excellent labels and carriers for designing of sensing devices [42,43]. In this line, complexes of NPs and biomolecules (e.g., peptides, proteins and nucleic acids) have been broadly utilized in many biosensors to detect and amplify bio-recognition events [44]. Nanoparticles contribute to the improvement of optical and electrochemical sensors performance in terms of sensitivity and selectivity, long life, and large surface area [36]. In electrochemical biosensors, the nanomaterials not only improve the charge and electron transmission but also provide low background current and high signal-to-noise ratios, leading to increase of electrochemical properties [45].

In the past decade, various biosensing methods have been established for monitoring and management of *H. pylori* infection including optical-based, mass-based and electrochemical-based biosensors [9]. A comparison between the LOD (limit of detection) and LR (linear range) of these reported biosensors is summarized in Table 1. Among the developed detection strategies, the DNA hybridization assays have played a significant role due to their repetitively, sensitively and selectively [46]. In addition, there have been many investigations on the integration of such biosensors with microfluidic platforms to develop user-friendly and rapid detection devices for point-of-care applications that was discussed in Section 3.

2.1. Optical-based H. pylori nano-biosensors

Optical-based biosensors are usually non-destructive to an analyte to be detected, and can be fabricated and manipulated relatively in an easy and rapid fashion [47]. Various optical detection methods including fluorescence, chemiluminescence (CL), colorimetry, SERS (surface-enhanced Raman scattering) and SPR (surface plasmon resonance) are extensively adopted for signal harvesting in nanosensors [48]. They employ nanomaterials owing to their ease of use and high sensitivity. In addition, nanomaterials usually amplify the original transduced weak signals by several orders of magnitude. This make the nanomaterial-based optical biosensors highly sensitive for biosensings [49,50]. In this section, to provide a better understanding of nanomaterial-based *H. pylori* optical biosensors (Table 1), the outstanding examples were summarized based on employed transducing methods.

Table 1
Linearity range (LR) and limit of detection (LOD) of different detection systems for diagnosis of *H. pylori*.

Detection method	Strategy	PCR amplification prior to detection	Detection time	LOD	Linear range	Ref.
Optical	FRET using CdTe QDs; QDs-(NH_2) oligonucleotide and Tamra-oligonucleotide hybridized to urease gene	+	~10 min	4.5×10^{-9} M	10–200 nM	[53]
	FRET based QD-aptasensor, DNA hybridization between ssDNA-QDs/GO system	+	~80 min	0.46×10^{-12} M	1.25–875 pmol/l	[58]
	Graphene-based interdigitated electrodes and an inductive coil antenna printed onto silk thin-film substrates	–	Not reported	~100 *H. pylori* cell	$100–10^6$ cfu/μl saliva	[61]
	Hybridization of cDNA with AuNPs-labeled probe and capture probe immobilized on self-assembly monolayer	+	~45 min	0.5 nM	Not reported	[65]
	Colorimetric assay based on AuNPs for ureC gene detection	+	~4 h	10 copies of the ureC gene	Not reported	[67]
	Colorimetric assay based on AuNPs for ureC gene detection	+	~1 h	10 CFU/mL	10–10,000 CFU/mL	[68]
	employing a unique monoclonal antibody against *H. pylori* urease and using a SPR apparatus	–	Not reported	2×10^7 bacteria/ml	Not reported	[71]
Piezoelectric		–	Not reported	Dilution 1/100 (serum)	100 to 500 mg Ag/ml	[75]
Electrochemical	a voltammetric enzyme-linked immunoassay for *H. pylori* specific IgG antibody using HRP and (TMB)-H_2O_2	–	Not reported	1.0 units/ml	0–100 units/ml	[78]
	DNA biosensor using phen-dione as the electrochemically active ligand in osmium complexes	+	~1 h	6×10^{-12} M	5–20 pmol	[79]
	Interactions between DNA and new electroactive Schiff base ligands	+	~1 h	8.3×10^{-6} M	8.9–22.2 μM	[80]
	DNA biosensor using a bismuth immobilized carbon nanotube electrode	+	~1 h	6.7×10^{-10} M		[9]
	Single-mismatch position-sensitive detection of DNA based on a ruthenium complex	+	~1 h	92×10^{-12} M	106–708 pmol	[83]
	Improved and sensitive genosensor using AuNPs and ruthenium complexes	+	~1 h	25×10^{-12} M	40–800 pmol	[84]
	intercalation of pentaamin ruthenium complex with Hairpin DNA modified on AuNPs	+	Not reported	1×10^{-15} M	down to 2×10^{-15}	[46]
	DNA biosensor based on proximity-dependent DNA ligation assays with DNAzyme amplification of hairpin substrate signal	+	~2 h	50×10^{-15} M	100 fM to 1 nM	[85]
	Immobilizing urease enzyme of *H. pylori* on PVC ammonium selective electrode by using nonactine as an ammonium ionophore	+	1–2 min	Not reported	1×10^{-5} to 1×10^{-2} M	[87]
	Immobilization of ssDNA probe on AuNPs and Oracet blue as a redox indicator	+	Not reported	0.17×10^{-9} M	0.3–240 nmol/L	[88]
	Immobilization of ssDNA probe on GO/AuNPs/GCE and Oracet blue as a redox indicator	+	~220 min	27.0 × 10–12 M	60.0–600.0 pM	[89]
Microfluidic	Microfluidic-based immunoassay by using PDMS/glass microchannels	–	~30 min	10 ng	10–1000 ng	[103]
	PDMS microchannel immunoassay with a RLS gold nanoparticle	–	~30 min	10 ng	10–1000 ng	[104]
	Microchip-based electrokinetically driven indirect immunoassay	–	~26 min	1 ng/μL	1–100 ng/μL	[105]
	Immobilized *H. pylori* antigen on an immuno-column incorporated into a flow-injection (FI) analytical system	–	~25 min	0.62 U/mL	0–100 U/mL	[108]
	microfluidic enzyme-linked-immunomagnetic assay coupled to a gold electrode using a non-competitive immunoassay	–	~25 min	0.37 U/mL	0–100 U/mL	[110]
	Laser-induced fluorescence integrated in a microfluidic immunosensor	–	~28 min	0.17 U/mL	0–100 U/mL	[107]
	An integrated microfluidic system for diagnosis of the resistance of *H. pylori* to quinolone-based antibiotics	+	~1 h	10 bacterial cells	$10–10^2$ bacterial cells	[112]
	Sample introduction interface for on-chip nucleic acid-based analysis	+	~7 min	Not reported	Not reported	[6]

2.1.1. *Fluorescence-based H. pylori nano-biosensors*

The functionalized nanomaterials with fluorescence emission have been extensively used to probe dynamic biological manners by means of electron-transfer quenching or FRET which depend on the energy transfer between two fluorescent molecules – donor and acceptor [51,52]. Optical-based biosensors usually have utilized FRET for the detection of different biomolecules such as proteins, nucleic acids, peptides and small molecules [53]. Based on different signal markers, various functionalized nanomaterials such as gold nanoparticles (AuNPs), quantum dots (QDs) and carbon nanomaterials such as graphene oxide (GO) have been widely used as donor or acceptor fluorophore [54,55]. These nanostructures have excellent fluorescent properties such as better stability, high spectral resolution, acutely sharp emission bands and high-throughput screening [54,56]. Nevertheless, intrinsic fluorescence of some proteins in serum may be interfered by outcome of the sensor. Application of fluorophores with time-resolved fluorescence properties can overcome this problem [57].

In recent years, fluorescent sensing platforms based on QDs as donor were established for the sensitive determination of specific sequence of *H. pylori* DNA [53,58]. QDs are fluorescent semiconductor nanocrystals which are composed of substances among II–VI, III–V and IV–VI elements [53]. QDs exhibit unique electro-optical and photophysical properties. These features offer numerous benefits over conventional dyes for sensing events for instance high quantum yield, constancy against photobleaching, wide-ranging absorption ranges and narrow emission spectra with large emission shifts [42,59]. Shanehsaz et al. developed a FRET based QD-biosensor which functioned using two oligonucleotide probes labeled with CdTe-QDs and 5-

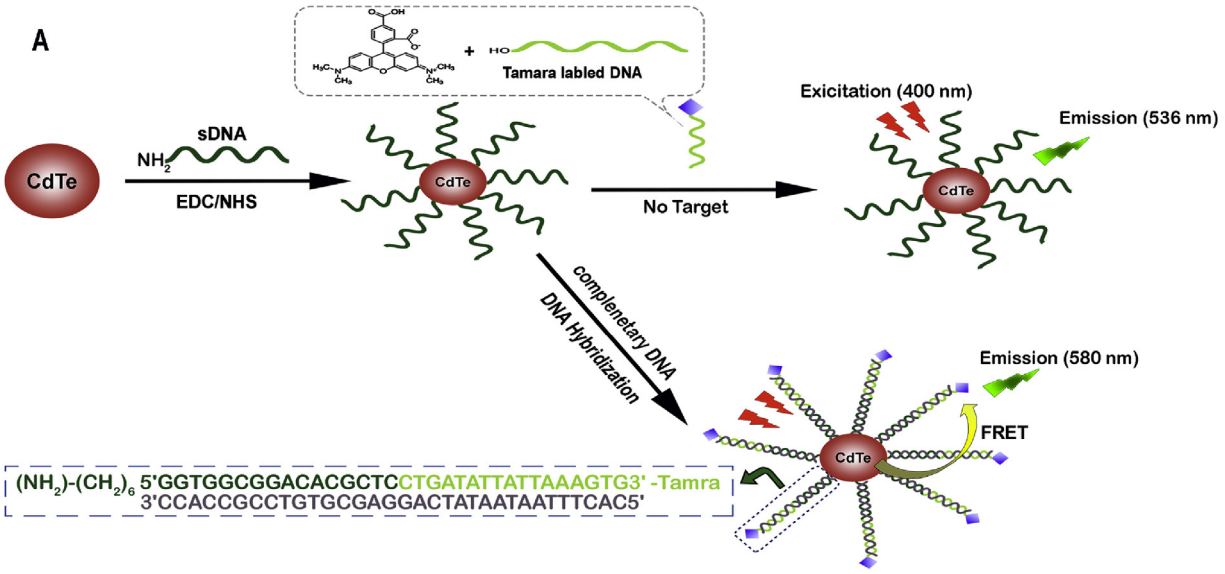
A
Tamara labled DNA
CdTe
sDNA
NH2
EDC/NHS
CdTe
No Target
Excitation (400 nm)
Emission (536 nm)
CdTe
complenetary DNA
DNA Hybridization
Emission (580 nm)
FRET
CdTe
(NH2)-(CH2)6 5'GGTGGCGGACACGCTCCTGATATTATTAAAGTG3' -Tamra
3'CCACCGCCTGTGCGAGGACTATAATAATTTCAC5'

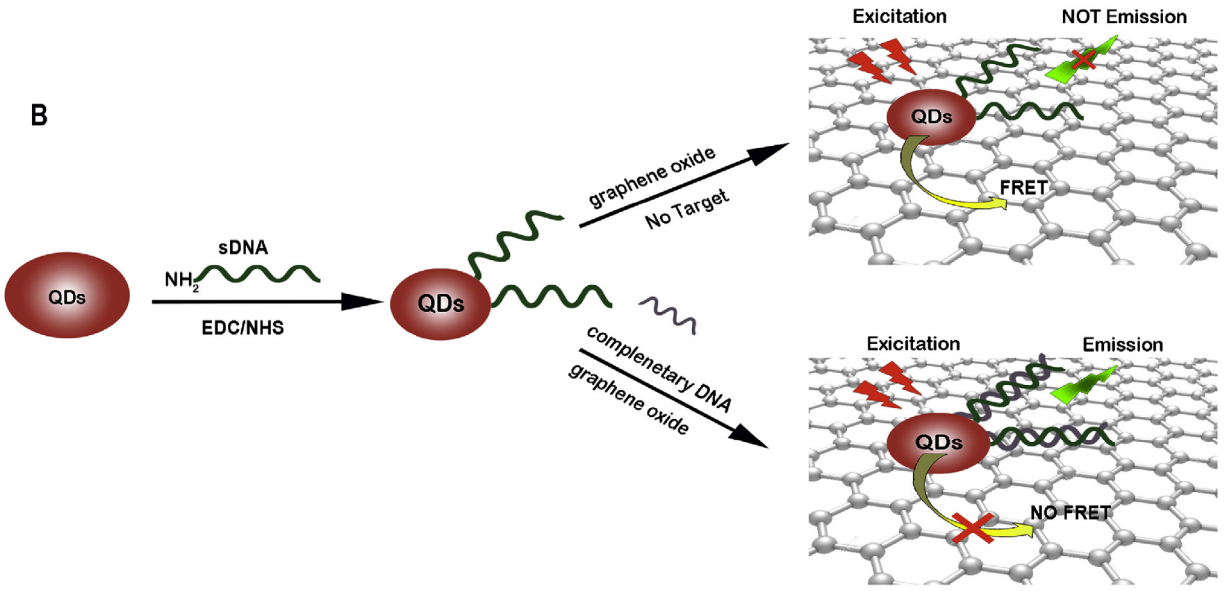
B
QDs
sDNA
NH2
EDC/NHS
QDs
graphene oxide
No Target
Excitation
NOT Emission
QDs
FRET
complenetary DNA
graphene oxide
Excitation
Emission
QDs
NO FRET

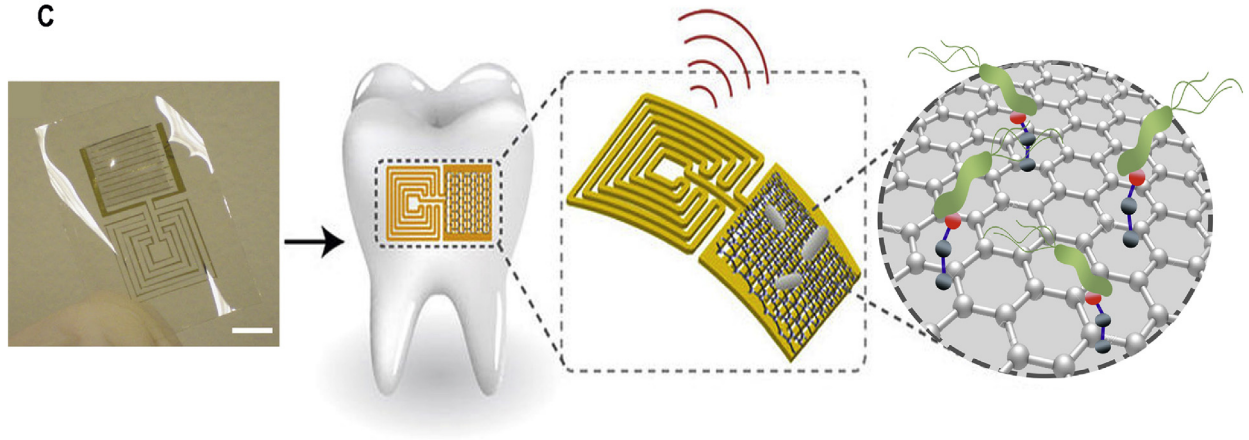
C

carboxytetramethylrhodamine (Tamra), respectively. QDs labeled with an amino-modified first oligonucleotide, and a Tamra-labeled second oligonucleotide was added to the DNA targets upon which hybridization occurred. After hybridization process, the FRET phenomena were appeared because of the close proximity of Tamra fluorophore (the acceptor) and the QDs (the donor), which cause the excitation of Tamra molecules. In the absence of target DNA, the probes are not ligated, and no emission by the Tamra fluorophore is produced due to the lack of FRET (Fig. 2A). This method simply and rapidly detected of a synthetic 210-mer nucleotide derived from Helicobacter on a nanomolar level with linearity range of 10–200 nM and LOD of 4.5 nM [53]. However, QDs have great advantages, modified or conjugated QDs commonly suffer from intrinsic limitations, such as complicated modification, potential toxicity, intrinsic blinking and chemical instability and low fluorescence. Modifications of biocompatibility, sizes, charges, stability, surface coating and core/shell structure are considered to be efficient solutions for QDs limitations [60].

Another FRET-based QD-aptasensor for ultrasensitive detection of *H. pylori* DNA was reported by Liu and Su [58] with a LOD of 0.46 pmol L^{-1} while the concentration of *H. pylori* DNA was within the range of 1.25–875 pmol L^{-1}. Their strategy for *H. pylori* detection was based on DNA hybridization between specific single-stranded DNA (ssDNA) as aptamer for *H. pylori* DNA and the complementary target *H. pylori* genomic DNA. Also graphene oxide was used as a *nanoscaffold* for ssDNA. Firstly, ssDNA-QDs genosensor was obtained by covalent reaction between the carboxy group of $CuInS_2$-QDs and the NH_2 group modified ssDNA in the presence of EDC and NHS. In the absence of the complementary target *H. pylori* DNA, GO could adsorb ssDNA-QDs DNA sensor and efficiently quench the fluorescence of ssDNA-QDs. While the complementary DNA as target was added, the ssDNA-QDs specially bound with the *H. pylori* DNA. The formation of dsDNA would change the conformation of ssDNA and disrupt the interaction between ssDNA and GO. Thus, the dsDNA-QDs/GO system exhibited a stronger fluorescence emission than that of the ssDNA-QDs/GO system (Fig. 2B).

In recent years, GO nanosheets, because of their unique characteristics, have been recognized as an efficient bioanalytical platform for *H. pylori* assays in human saliva (Fig. 2C). In this platform, the wireless graphene sensor was bio-transferred onto the surface of a tooth. For detection purposes, the alterations of graphene resistance versus quantity of *H. pylori* were analyzed [61]. Required high skills for the construction of GO nanosheets as well as alteration of the sensitivity of the sensing platform by interaction of serum proteins with GO are some drawbacks of biosensing methods employing GO. Pretreatment of GO with molecules like albumin or PEG may be alternative strategies to overcome this limitations [62].

2.1.2. Colorimetric H. pylori nano-biosensors

Metal nanoparticles are appropriate candidates for colorimetric assays because of having size-/distance-dependent optical properties. For instance, the colors of colloidal AuNPs, which change in the inter-particle plasmon coupling and resulting in surface plasmon band shift, are sensitive to their aggregation/dispersion. Moreover, extinction coefficient of AuNPs is over 1000 times higher than that of organic dyes, which offers high sensitivity for AuNPs-based colorimetric biosensors [63,64]. Owing to unique properties of metal nanoparticles, a novel colorimetric nanobiosensor for sensitive determination of the *H. pylori* genome using AuNPs-labeled probe was reported [65]. Based on a cDNA region of the urease gene, two specific thiol-modified capture and signal probes were planned. Firstly, AuNPs were immobilized on an APTES-activated glass by the self-assembly method. Afterwards, the capture probe was immobilized on AuNPs, and the signal probe was labeled with different AuNPs as well. The hybridization of the two probes and the cDNA over the glass surface in the presence of cDNA in the reaction mixture led to a reduction in the optical density of AuNPs signal, which was proportional to the cDNA concentration (Fig. 3A). The limit of detection was measured as 0.5 nM. It should be noticed when AuNPs-based sensors use for detection of targets in complex samples like serum, a problem called “corona shield effect” usually appear. The use of PEG molecules in the construction of biosensors can address this issue [66].

An enzyme-linked immunosorbent assay (ELISA) of thermophilic helicase-dependent isothermal DNA amplification (tHDA) was developed for the detection of *H. pylori*. The amplification of bacterial DNA was performed by the isothermal digoxigenin (DIG)-labeling tHDA manner via primers targeting ureC, led to the accumulation of DIG-labeled DNA amplicons. The amplicons were denatured using heat and then associated with complement biotinylated capture probe. The hybrid was transferred to streptavidin-coated microtiter plate for immobilization. Finally, the developed color was measured at 405 nm by the adding of an anti-DIG antibody HRP (horseradish peroxidase) conjugate and 2,2-azino-di- (3-ethylbenzthiazolinsulfonate) substrate solution (Fig. 3B) [67]. Results obtained by testing dilutions of *H. pylori* detected 10 copies of the ureC gene. In a similar manner, a nano-diagnostic method using the tHDA reaction and immobilizing of ureC gene probes on Au-NP were used. The accumulated DNA amplicons was hybridized with specific gold nanoparticle probes. The hybridizing process was assembled of AuNPs give rise to a purple color that was colorimetrically detected. On the contrary, for the unbound probes, a red color of separated AuNPs was observed (Fig. 3C). Using this method, they detected as little as 10 CFU mL^{-1} of *H. pylori* within less than 1 h [68].

2.1.3. Surface plasmon resonance H. pylori nano-biosensors

Surface plasmon resonance (SPR) biosensors as very powerful tools are widely used to detect biomolecular interactions (e.g. specific binding of analytes). SPR has inherent advantages of being high-throughput, real-time, and label-free technique for measurement of binding kinetics and affinity [69]. When a biomolecular interaction takes place on gold thin film, the refractive index in the vicinity of the surface is altered. This shift of refractive index can be sensed by the SPR sensor [70]. SPR has successfully been applied to detection of *H. pylori* by means of immunoreactions. Nishimura et al. by employing a unique monoclonal antibody against *H. pylori* urease and using a SPR apparatus, detected down to 2×10^7 bacteria/ml. In this platform, the extensive concentration of *H. pylori* could be detected comparing with the conventional assay kit, while the detection limit of the SPR system was less by 10 fold [71]. Heparin/heparan sulfate (H/HS) binding properties of *H. pylori* VacA 58-kDa subunit were determined by in-silico and SPR-based biosensor studies [72]. A SPR and isothermal titration calorimetry systems developed by Fabina et al. to monitor the Ni(II)-dependent binding of *H. pylori* NikR (HpNikR) to DNA. NikR is a transcription

Fig. 2. Examples of optical nanosensors developed for *H. pylori* determination. (A) Schematic representation of a nanobiosensor for detection of *H. pylori* based on a FRET system using the QDs-(N)DNA as a donor and the (T)-DNA as an acceptor. In the absence of the complementary DNA, PL emission of QDs was observed at 536 nm with an excitation at 400 nm. Presence of complementary DNA led to the emission of the system showed a red shift around 580 nm via FRET phenomena. (B) Schematic illustration of the ssDNA-QDs/GO-based sensing system for *H. pylori* DNA detection. (C) Optical image of the graphene wireless sensor biotransferred onto the surface of a tooth. Reproduced from published papers [53,58,61].

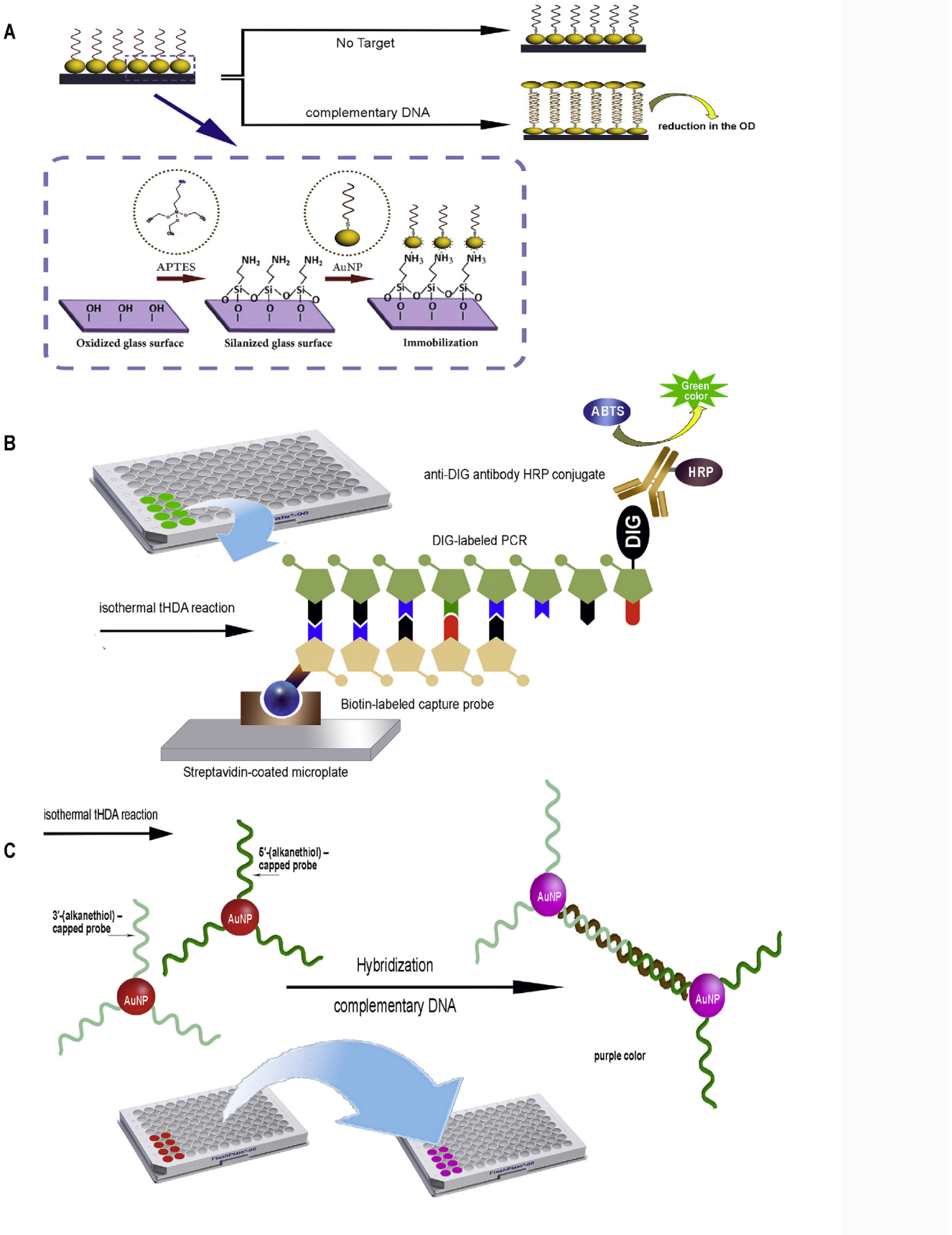

Fig. 3. (A) Optics-based nanobiosensor for determination of the *H. pylori* genome using a gold nanoparticle. (B) Colorimetric biosensors proposed for *H. pylori* determination based on ELISA of DIG-labeled tHDA amplicons. (C) A schematic demonstrating visual detection of *H. pylori* using red to purple color change of gold nanoparticles. Reproduced from published papers [65,67,68].

factor that regulates the expression of Ni(II)-dependent enzymes. The expression of *H. pylori* urease enzyme prevented by interaction of the Ni(II)-loaded HpNikR with dsDNA operator region of the urease promoter (OP_{ureA}). A sensor chip surface bearing immobilized dsDNA OP_{ureA} was prepared by affinity-capture technique and affinity of the transcription factor for its region was assessed in the SPR experiments. The SPR assay developed and validated in this study constitutes a suitable method to display potential drug lead candidates acting as inhibitors of this protein–dsDNA interaction [73]. The significant limitations of SPR include cross-sensitivity to structurally similar but non-target molecule, non-specific interaction between the sensor surface and non-target molecules, and background refractive index alteration owing to sample temperature and composition oscillation [74].

2.2. Piezoelectric-based H. pylori nano-biosensor

Piezoelectric biosensors are considered as mass measurement devices which rely on detecting the change of resonance frequency on a quartz crystal microbalance (QCM). The change in the oscillation frequency of the QCM device is proportional to any changes induced by mass binding to the electrode. The use of QCM allows for the detection of pathogens using probes modified with immobilized antibodies [70]. A sandwich and enzymatically amplified piezoelectric biosensor was established for the detection of *H. pylori* antibody. In this platform, recombinant *H. pylori* antigens were immobilized onto the surface of AT-cut quartz crystals (10 MHz) as reaction carrier to capture the associated antibodies. Following incubation with positive human serum samples with very low antibody titer, a less significant signal was obtained compared with the negative background. In order to increase the positive signal and reduce the negative background, incubation was followed with anti-human IgG. The binding of anti-human IgG to IgG antibodies resulted in a sandwich immunocomplex. Since the binding of the secondary antibody was only observed when patient sera were *H. pylori* positive, the total frequency changes and positive-to-negative signal ratio were increased. Once enzyme (HRP or AP) conjugated antibodies used, the sandwiched complexes were exposed to associated substrates. Deposition of precipitates on the crystal surface, following the enzymatic reaction, resulted in greater sensitivity [75]. By means of this strategy, human serum could be detected as positive in a dilution of 1/100.

2.3. Electrochemical-based H. pylori nano-biosensors

Function of electrochemical biosensors relies on pairing a biological substance to an electrode transducer [76]. Electrochemical-based biosensors have shown fascinating properties over optical-based ones. In reverse of optical mechanisms that are commonly costly with low portability, electrochemical-based biosensors are more practical for field-deployable applications. Such sensors require low amount of sample/reagent volumes without any need to fluorescent labels resulting in low cost of operation and primary investment for equipment [76,77].

In recent years, several biosensors for *H. pylori* detection have been developed based on various electrochemical methods including electrochemical impedance spectroscopy (EIS), differential pulse voltammetry (DPV) as well square-wave voltammetry (SWV) (Table 1). He et al. designed a voltammetric enzyme-linked immunoassay for *H. pylori* specific IgG antibody using HRP as labeled enzyme and Tetramethylbenzidine (TMB)-H_2O_2 as substrate. The enzymatic product is electroactive and exhibits a sensitive DPV response at 0.1 V (versus Ag/AgCl) in acetate buffer solution with pH 4.0. The detection limit for *H. pylori* specific IgG antibody was 1.0 units ml^{-1}, which was about seven times lower than that of sensed by traditional spectrophotometric ELISA method [78].

Majority of the electrochemical indicators developed for electrochemical biosensors have been fabricated by immobilization of a thiolated capture probe sequence from *H. pylori* through S–Au bonds onto gold. In these sensing platforms, a simple and reagent saving method of the interactions of DNA with redox-active phendione of osmium complexes was described by Del pozo et al. [79]. In this study, gold electrodes were modified with DNA via adsorption of $[Os(bpy)_2(phe\text{-}dione)]^{3+/2+}$ (bpy = 2,2′-bipyridyl) or $[Os(phen)_2(phen\text{-}dione)]^{3+/2+}$ (phen = 1,10-phenantroline) as electrochemical reported molecules. Following hybridization of the complementary DNA sequence with immobilized single-stranded *H. pylori* DNA probe onto a gold electrode, the osmium complex was electrochemically accumulated within the double-stranded DNA layer (Fig. 4A). Electrochemical detection was performed by DPV over the potential range where the quinone moiety of the phendione ligand was redox active. Employing this approach, a sequence of the *H. pylori* could be quantified over the range from 5 to 20 pmol with a detection limit of ~6 pmol [79]. In another study, a biosensor was employed as an electrochemical indicator to detect hybridization of a molecule containing ortho quinone functional group [N,N′-Bis(3,4-dihydroxybenzylidene)-1,2-diaminobenzene (3,4-DHS)] (Fig. 4A). After hybridization, 3,4-DHS was accumulated and observed by DPV. The linear range of complementary target sequence of *H. pylori* was 8.9–22.2 μmol L^{-1}, with a detection limit of 8.3 ± 0.4 μmol L^{-1} [80].

Carbon nanotubes (CNTs) also have been employed for the fabrication of an electrochemical biosensor for *H. pylori* detection. Owing to its electrocatalytic property and high electrical conductivity, CNTs can promote electron transfer and provide a large cylindrical surface area [81,82]. In this aspect, Ly et al. investigated a voltammetric assay of *H. pylori* DNA using a bismuth-immobilized carbon nanotube electrode (BCNE). The analytical cyclic voltammetry (CV) peak potential was obtained at a 0.4 V reduction scan, where the diagnostic optimum square-wave (SW) stripping working range was achieved at 0.72–7.92 μg/mL *H. pylori* DNA (11 points). The results showed that under optimum conditions, a detection limit of 0.06 μg/mL was obtained within two minutes as the duration of sensing [9].

In a study, Garcia et al. showed that pentaamin ruthenium [3-(2-phenanthren-9-yl-vinyl)-pyridine] complex (Fig. 4A), owing to its intercalating characteristics, was able to bind to double stranded DNAs more efficiently rather than to single stranded DNAs previously immobilized onto the gold electrode surface [83]. In another study conducted by the same group, they improved a new strategy along DNA-sensing platforms with genosensor applications. To implement this system, they employed combination of AuNPs with pentaamin ruthenium $(Ru(NH_3)5_L)^{2+}$ complex as a redox center that can be used as electrochemical indicator of the hybridization event. With the purpose of assessing the possibility of these planning as DNA-sensing devices, a thiolated capture probe sequence from *H. pylori* was immobilized onto the Au surface. The hybridization event was detected using a water-soluble pentaamin ruthenium complex (Fig. 4A). On the basis of this approach, complementary target sequences of *H. pylori* were detected over the range of 40–800 pmol with a detection limit of 25 ± 2 pmol [84].

In a similar manner, Hui-Fang Cui et al. developed a method based on intercalation of pentaamin ruthenium complex with Hairpin DNA (hpDNA) modified on AuNPs. At the first step, hpDNA was conjugated to AuNPs and a reporter DNA (rpDNA) to form hpDNA/AuNP/rpDNA nanoparticles. The rpDNA is complementary to about a half portion of the target DNA sequence (tDNA). In the next step, a capture DNA probe (cpDNA), complementary to the other half of the tDNA, was immobilized on the surface of a gold

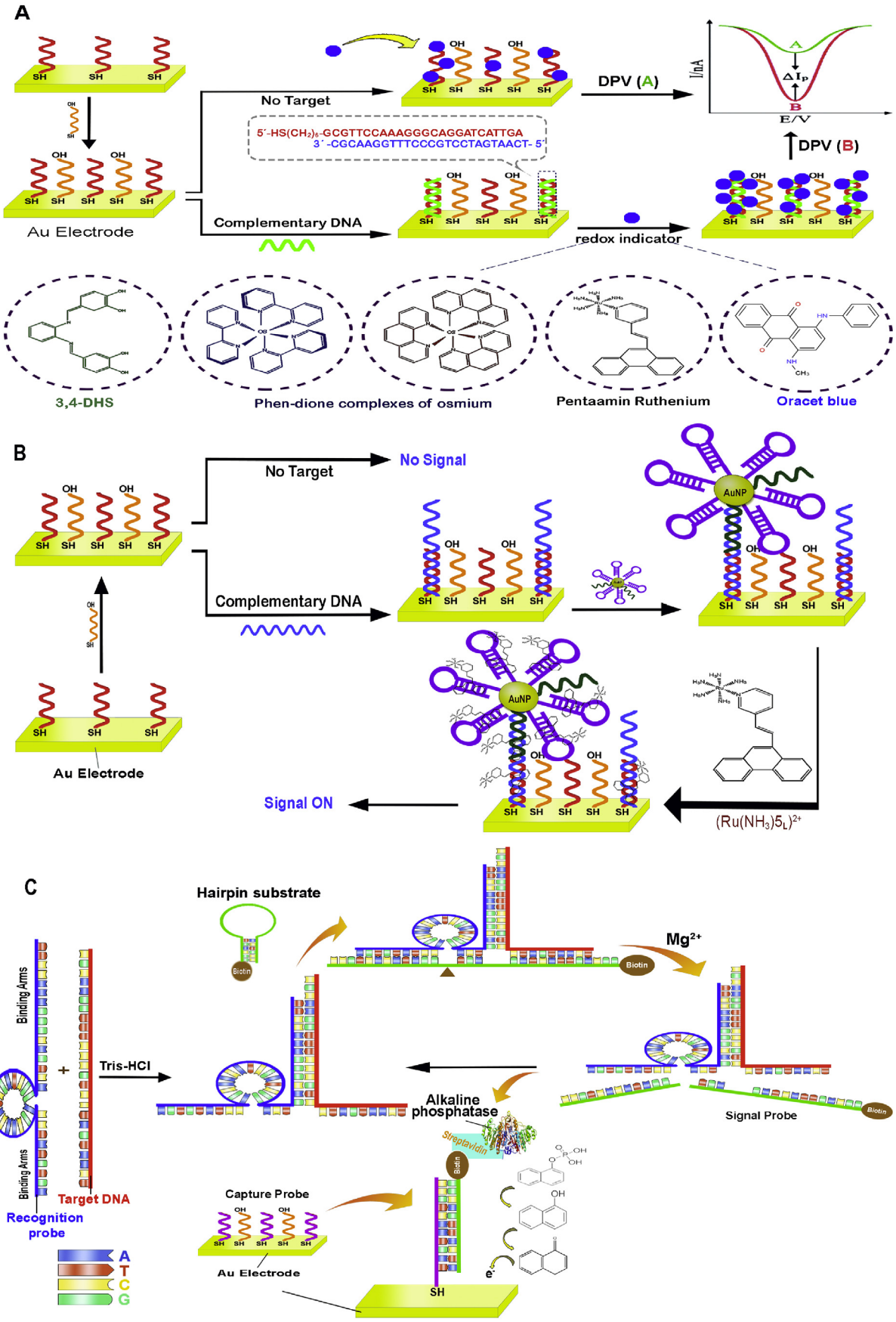
A
No Target
DPV (A)
I/nA
E/V
DPV (B)
5´-HS(CH2)6-GCGTTCCAAAGGGCAGGATCATTGA
3´ -CGCAAGGTTTCCCGTCCTAGTAACT- 5´
Au Electrode
Complementary DNA
redox indicator
3,4-DHS
Phen-dione complexes of osmium
Pentaamin Ruthenium
Oracet blue
B
No Target
No Signal
Complementary DNA
AuNP
Au Electrode
Signal ON
(Ru(NH3)5L)2+
C
Hairpin substrate
Biotin
Mg2+
Binding Arms
Tris-HCl
Alkaline phosphatase
Streptavidin
Signal Probe
Capture Probe
Target DNA
Recognition probe
Au Electrode
A
T
C
G

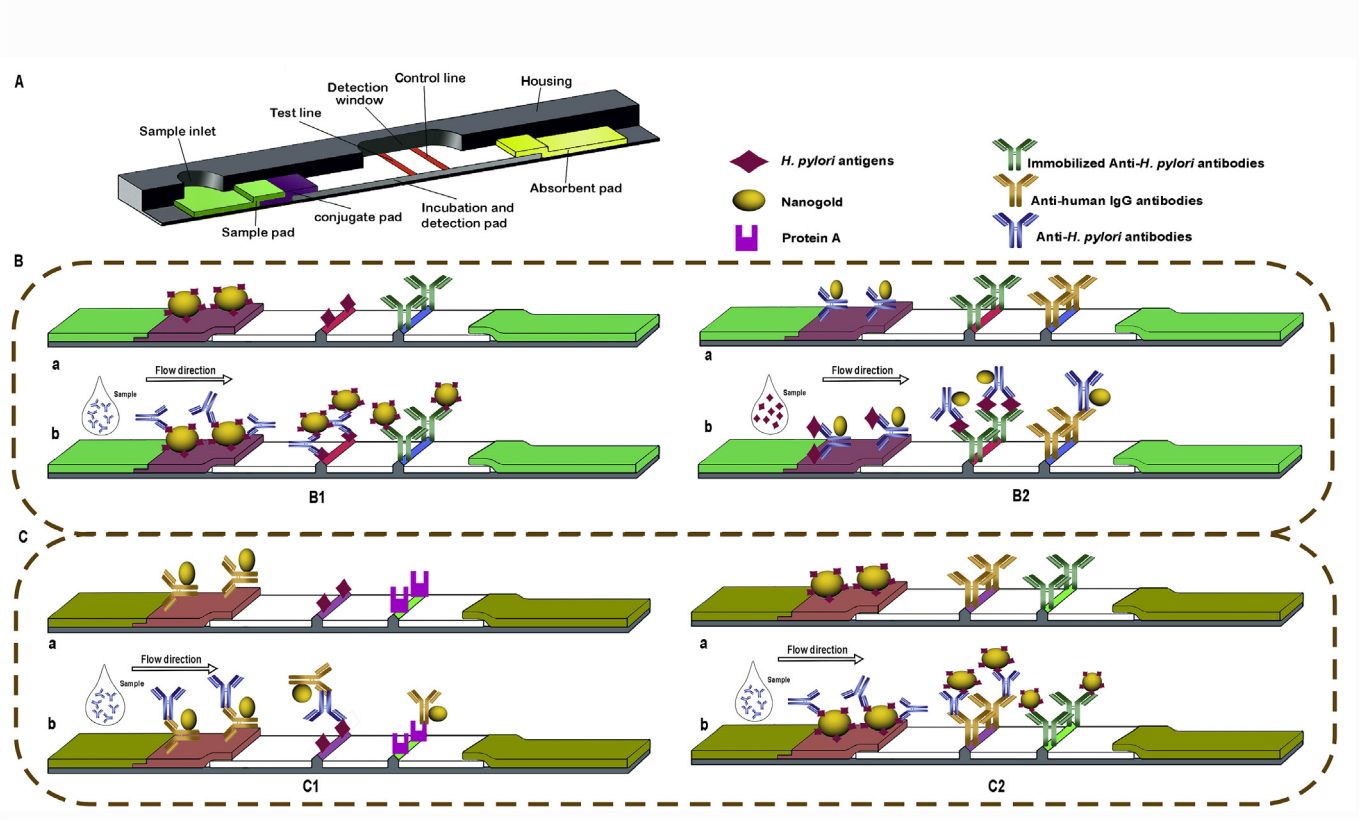

Fig. 5. (A) Schematic architecture and operation of lateral flow assay (test strip) for the diagnosis of *H. pylori* infection. (B) Sandwich format for the detection of anti-*H. pylori* antibodies (B1) and the detection of antigens (B2). (C) Indirect format for the detection of anti-*H. pylori* antibodies using antigen immobilized (C1) and antibody immobilized on the test line (C2). In all schemes, (a) and (b) refer to the constituents of the strip before and after the sample introduction to the strip, respectively.

electrode. After introduction of tDNA, a sandwich structure of (hpDNA/AuNP/rpDNA)/tDNA/cpDNA was formed on the electrode surface. The operation of DPV sensorgram was based on binding ruthenium with the hpDNA and the dsDNA of the sandwich structure. The sensitivity and selectivity of the DNA sensors was highly improved by several factors including high density of hpDNA on the surface of AuNPs and multiple ruthenium complex molecules intercalated with each hpDNA and dsDNA molecules (Fig. 4B). The DNA sensor exhibited a detection limit of 1×10^{-15} M (i.e. 1 fM), the DNA levels in physiological samples, with linearity down to 2×10^{-15} M. The sensor can distinguish even one single mismatched DNA from the paired tDNA [46].

Sun et al. [85], for the first time, reported a novel electrochemical DNA sensor for simple, sensitive and specific analysis of nucleic acids. The method relied on proximity-dependent DNA ligation assays with the DNAzyme amplification of hairpin substrate signal. DNAzymes and RNAzymes are examples of catalytic nucleic acids, representative of the allosteric aptamers suitable for the construction of biosensors. In these platforms, they could combine recognition units and amplifying readout units [86]. The central catalytic loop flanking the two binding arm are generally two functional domains of DNAzymes. Compared to optical DNAzyme sensors, however, electrochemical DNAzyme sensors still need more developments to be employed for practical applications. In the present work [85], a long DNA strand contains the catalytic motif of Mg^{2+}-dependent 10–23 DNAzyme, acting as the recognition probe. In the presence of the target DNA, part of it was complementary to 5′-end of the recognition probe. The results in the ligation of a stable duplex, and the unbounded part of the target DNA acted as one binding arm for the DNAzyme. This duplex, containing a complete DNAzyme sequence, could cleave the purine–pyrimidine cleavage site of the hairpin substrate. It resulted in breaking up the hairpin structure and the release of two single-stranded nucleic acids, one of which was biotinylated and acted as the signal probe. An immobilized thiolated capture probe could bind with the signal probe, employing biotin as a tracer, and streptavidin–alkaline phosphatase (SA–ALP) as a reporter molecule. The amount of 1-naphthol, generated through dephosphorylation of 1-naphthyl phosphate by the immobilized enzyme in 5 min, was voltammetrically determined (Fig. 4C). The results revealed that the sensor showed high sensitivity for complementary target sequences of *H. pylori* detection in a concentration range from 100 fM to 1 nM, with a detection limit of 50 fM. In addition, the sensing system showed a sensitive and reproducible response for the discrimination of the complementary sequence from mismatched sequences.

Urease is produced in abundance by *H. pylori*, increases urea levels in the gastric mucosa [1]. Owing to this fact, a urea biosensor was fabricated by immobilizing urease enzyme, obtained from *H. pylori*, on polyvinylchloride (PVC) ammonium selective electrode

Fig. 4. Electrochemical-based biosensors by DPV detection. (A) A schematic of the biosensors function based on redox-active indicators [3,4 DHS [80], phen-dione complexes of osmium [79], pentaamin ruthenium [83], Oracet blue [88,89]] strategy with binding to double stranded DNAs more efficiently rather than to single stranded DNAs. (B) The fabrication processes for the hpDNA based sandwich DNA sensor and the signal detection strategy. Reproduce from published paper [84]. (C) Schematic drawing of the setup for the recognition and electrochemical detection of the target DNA sequence based on DNAzyme amplification of hairpin substrate signal. Reproduced from published paper [85].

using nonactine as an ammonium ionophore. The effects of urease concentration, stirring rate and enzyme immobilization procedure on sensor response were investigated. The linear working range of the biosensor was from 1×10^{-5} M to 1×10^{-2} M with dynamic stability over 2 months with a response time of 1–2 min [87].

Recently, Oracet blue (OB) was employed as a redox indicator for amplifying the electrochemical signal of *H. pylori* DNA (Fig. 4A) due to its electrochemical properties [88]. OB is an anthraquinone derivative, which can be assumed as quinine. It is recognized that anthraquinone derivatives can be quite permanently perpetual active in the electrocatalytic redox reactions of different analytes [88,89]. In these works, a hybridization reaction was conducted with the target DNA and the immobilized DNA and DPV were used to monitor DNA hybridization by measuring the differences between the voltammetric signals of the OB obtained from different hybridization samples (non-complementary, mismatch and complementary DNAs). In another investigation, a single–stranded DNA probe was covalently immobilized on the surface of a gold electrode (AuE). The results showed that under optimum conditions, the electrochemical signal had a linear relationship with the concentration of the target DNA ranging from 0.3 nmol L^{-1} to 240.0 nmol L^{-1}, and the detection limit was 0.17 nmol L^{-1}, with a promising reproducibility and repeatability [88]. In another study, single-stranded DNA probe was immobilized on graphene oxide/gold nanoparticles modified glassy carbon electrode (GO/AuNPs/GCE). The result of this investigation demonstrated that this structure enhanced sensitivity and selectivity of *H. pylori* detection with a linear range of 60.0–600.0 pM and a LOD of 27.0 pM [89].

2.4. Paper-based H. pylori nano-biosensors

Although nanomaterial-based biosensors bring numerous benefits for detection purposes, there are still critical requirements to be addressed to develop affordable, portable and low-cost biosensors for point-of-care (POC) and field-deployable applications.

Paper-based biosensors provide a bridge twixt experimental platforms and the implementation of biosensors to perform affordable, easy-to-use and rapid diagnostics. Paper is a cheap and easy-to-access material and can be disposed or burned easily. Also, biosensing and recognition compounds can be easily mounted on paper through immunoreactions or nucleic acid hybridizations to make compact, low-cost and stable performance over a wide range of time and temperature [90,91]. The paper-based biosensors can be mainly divided into three categories: the dipstick assays, lateral flow assays (LFA) and the microfluidic paper-based analytical devices (μPADs). The dipstick assays, such as pH test strips, are the simplest ones, since they are based on the blotting of the sample onto a paper containing pre-stored reagents. However, the implementation of sophisticated fluidic manipulation on paper strips for detection assays can be challenging [37,90] and require careful considerations for precise liquid handling and distribution.

The LFAs, similar to dipstick, have all required reagents pre-immobilized within the strip. A liquid sample containing an analyte can flow through different regions of the strip, through the capillarity, conducting different steps of a desired detection assay [92].

In particular, a LFA (also called immunochromatographic assay) is generally made of four sections: a sample pad (cellulose), a conjugation pad (glass fiber), a detection pad (nitrocellulose membrane) and a wicking or absorbent pad (cellulose) (Fig. 5A). When an assay is performed, a small volume of liquid sample, containing an analyte, is introduced into the sample pad. The liquid then flows toward the conjugate pad where labeled biorecognition molecules are dispensed. In this pad, the binding reaction between the labels and the analyte occurs. In the detection pad, where reaction and detection during the assay happens, capture reagents are fixed to form test and control lines and the signal is developed. The function of the absorbent pad is to maintain a flow rate of the liquid sample over the membrane and avoids back flow of the sample. The main problems of the LFAs are the difficulty in performing multiplex and quantitative analyses [37,93]. To address such disadvantages, many investigations have been devoted to the development of μPADs, which will be reviewed in Section 3.

Implementation of NPs with LFAs and paper microfluidic devices, can improve the selectivity and sensitivity of these sensing platforms dramatically [93]. Various nanomaterials have been employed in LFAs for their unique electronic, optical, and/or structural properties. QDs and AuNPs are the most common materials used in paper biosensors [90].

The several LFA strips base on AuNPs are currently commercially available for *H. pylori* infection diagnosis (Table 2). Karakus and

Table 2
Principle and performance of commercially available lateral flow test strips based on gold nanoparticle for the detection of *H. pylori* in real samples.

Recognition base[a]	Assay format	Commercial tests	Sample	Detection time
Antibodies	Sandwich	OneStep *H. pylori* RapiCard™	Serum, whole blood	within 4–7 min
		INSTANT-VIEW® *H. pylori*	Whole blood	2–3 min
		BioSign® *H. pylori*	Serum	10 min
		Clarity *H. pylori*	Whole blood, serum, plasma	5 min
		BioStar® Acceava® *H. pylori*		10 min
		ICON® HP-One-Step		10 min
		QuickVue™ *H. pylori*		5 min or less
		Immunospec *H. pylori*		After 10 min
		SureStep™ *H. pylori*		1–5 min
		NOVAtest® One-Step *H. pylori*		Reported as fast
		Accu-Tell® Rapid *H. pylori*		Within 10 min
		RTA Labs *H. pylori* Test		Within 10 min
	Indirect	RAPIRUN *H. pylori*	Urine-based	10–20 min
		ASSURE® *H. pylori*	Whole blood, serum, plasma	After 15 min
Antigens	Sandwich	Immunospec *H. pylori* Antigen	Stool	10–15 min
		OneStep *H. pylori* Antigen		Within 15 min
		HELISTOOL *H. pylori*		10 min
		BIONEXIA® *H. pylori* Ag		Only 10 min
		H. pylori Stool Antigen (HPSA®)		10 min
		RAPID Hp StAR™		Within 5 min
		SD BIOLINE *H. pylori* Ag		10–15 min
		H. pylori Ag card test		5–10 min

[a] The information was gathered from the manufacturers' data sheet and published paper [94].

Salih compared and discussed on the components and the operation principles of lateral flow immunoassay (LFIA) devices for rapid *H. pylori* detection [94]. These devices are particularly used either to detect *H. pylori* antigens in stool samples or to detect anti *H. pylori* antibodies in blood samples, e.g. whole blood, serum and/or plasma. These test strips are available in "sandwich" and "indirect" or competitive formats, in which antigens or antibodies can be immobilized on the test line as shown in Fig. 5B–C. In the presence of analyte in sample, two red lines appear at test and control lines, while in the absence of the analyte, only one red line as control emerges.

To fabricate biosensors in sandwich format for the detection of anti-*H. pylori* antibodies (Fig. 5-B1), *H. pylori* antigens are immobilized on AuNPs located within the conjugate pad. *H. pylori* unlabeled antigens are coated on the test line and similarly anti-*H. pylori* antibodies are immobilized on the control line. In the presence of a sample solution, anti-*H. pylori* antibodies and labeled antigens form complexes in the conjugation pad, which they continue to migrate with the fluid flow. The complexes are captured at the test line via binding to the immobilized unlabeled antigen. The flow of the sample fluid continue toward the control line where the remaining antigen coated AuNPs will bind to the immobilized anti-*H. pylori* antibodies and produce a red line. To develop test strips for the detection of *H. pylori* antigens (Fig. 5-B2), anti-*H. pylori* antibodies coated on AuNPs are placed within the conjugate pad, while another anti-*H. pylori* antibodies and similarly anti-IgG antibodies are immobilized on the test line and the control line, respectively. The addition of a sample drop onto the sample pad leads to migration and interaction between antigens and the antibodies coated on AuNPs. The produced complex subsequently migrates to the other parts of the test strip. At test line, analyte binds to the immobilized antibody and at control line it binds to the immobilized anti-IgG antibodies results in emerging two red lines [37,94].

As for lateral flow assays with antibody coated indirect format (Fig. 5-C1), *H. pylori* antigens coated on AuNPs are laid into the conjugate pad, anti-human IgG antibodies are immobilized on the test line and similarly anti-*H. pylori* antibodies are immobilized on the control line. The introduction of a sample drop onto the sample pad leads to migration and interaction between antibody and the antigens coated on AuNPs. The complex subsequently migrates to the other parts of the strip. At the test line, the complex binds to the immobilized antibody while at the control line it binds to the immobilized anti-*H. pylori* antibodies results in production of two red lines. In the antigen coated indirect format (Fig. 5-C2), at the conjugate pad, anti-human IgG antibodies coated on AuNPs are immobilized, while *H. pylori* unlabeled antigens are immobilized on the test line. Similarly, proteins A are immobilized on the control line. After sample introduction to the sample pad, analytes start flowing toward the conjugate pad where they bind to the antibodies coated on AuNPs. When complex sample reaches at the test line, it binds to immobilized unlabeled antigen. The flow of the sample fluid will continue toward the control line where the remaining immune-complexes will bind to the immobilized protein A and produce a red color line. This line will turn positive even the sample does not contain antibodies to *H. pylori* since the gold labeled anti-human IgG antibodies would bind to protein A [94].

3. Microfluidic-based detection of *H. pylori*

The miniaturization of laboratory processes offers substantial advantages over traditional techniques in terms of cost, process time and potential for high throughput analysis and automation. Microfluidics has been recognized as an expanding technology to realize POC diagnostics to address global health issues. Owing to their miniaturization and flexibility in design and operation they can meet ASSURED criteria, established by The World Health Organization (WHO) [37,38]. Assured stands for **a**ffordable, **s**ensitive, **s**pecific, **u**ser friendly, **r**apid and robust, **e**quipment-free, and **d**eliverable to end-users technologies suitable to address global health issues.

Microfluidics, integrated with different functional units (e.g., pumps, valves and reactors) can be employed to fabricate miniaturized analytical system [95] to process small sample volumes [96,97]. Thus, microfluidic devices significantly decrease the consumption of samples and reagents [98], the complexity of operation processes, and the assay time without compromising specificity and sensitivity [99]. Microfluidic-based diagnostic devices are able to process and analyze a wide spectrum of clinical samples, such as blood, oral fluid/saliva and urine [100]. Transport of fluid in these miniaturized systems can be realized in passive mode without any energy consumption (e.g., gravity, surface tension, capillary forces), and active mode of operation once an energy-consuming microdevice (e.g., micro pump, electric force, and centrifugal force) is employed.

Integration of immunoassay onto microfluidic devices led to the advent of lab-on-a-chip or micro-total analysis systems (μ-TAS) to reduce reaction and assay time [101,102]. In a lab-on-a-chip device, the specific *H. pylori* antigens are immobilized on the wall of a microchannel. Based on this framework, Lin et al. developed a microfluidic-based immunoassay for the detection of *H. pylori* infection using poly(dimethylsiloxane) (PDMS)/glass microchannels and compared the results with conventional nitrocellulose membrane-based dot-ELISA. The microchannel immunoassay validly detected *H. pylori* antigens in quantities on the order of 10 ng, which provides a sensitivity of detection comparable to conventional dot-blot measurement with a sensitivity and specificity of 100% and 90%, respectively. Volume of sample solutions were 100-fold less in comparison to conventional procedures [103]. In a similar manner, a PDMS microchannel immunoassay has been developed with a resonance light scattering (RLS) gold nanoparticle visualized by using dark-field microscopy for the detection of *H. pylori* and *E. coli* O157:H7. The aim of this study was to recognize particular antigens of *H. pylori* with biotinylated polyclonal antibodies without the intervention of sophisticated instruments. Gold particles functionalized with a secondary antibiotin antibody were then used as the readout. A colorimetric quantification scheme was developed for the detection of the visual color changes raised from immune reactions in the microchannel. The microchannel immunoassay reliably detected *H. pylori* antigens in quantities on the order of 10 ng. In addition, the nanoparticles within the microchannels could be stored for at least 8 months without any loss in signal intensity [104]. Another microchip-based electrokinetically driven indirect immunoassay for *H. pylori* detection was developed by the Gao et al. [105]. The H-shaped microchip was made of PDMS/glass using photolithography and replica molding (Fig. 6A). Their method was based on the immunoreaction between the anti-*H. pylori* antibody and the bacterial antigen coated on the wall of the microchannel with minimal amount of reagents (12 μL). This reaction resulted in production of fluorescence signal. Rhodamine-labeled secondary antibodies were employed for signal generation (Fig. 6-B1). They obtained a LOD of 1 ng μL^{-1} in about 26 min reaction period [105,106]. The detection limit was lower than that of obtained from previous pressure-driven ELISA [104] using colorimetric detection (4 ng μL^{-1}) or conventional dot–blot ELISA (10 ng μL^{-1}).

With further development on automatic control and detection strategy, in a series of platforms, immunological interactions

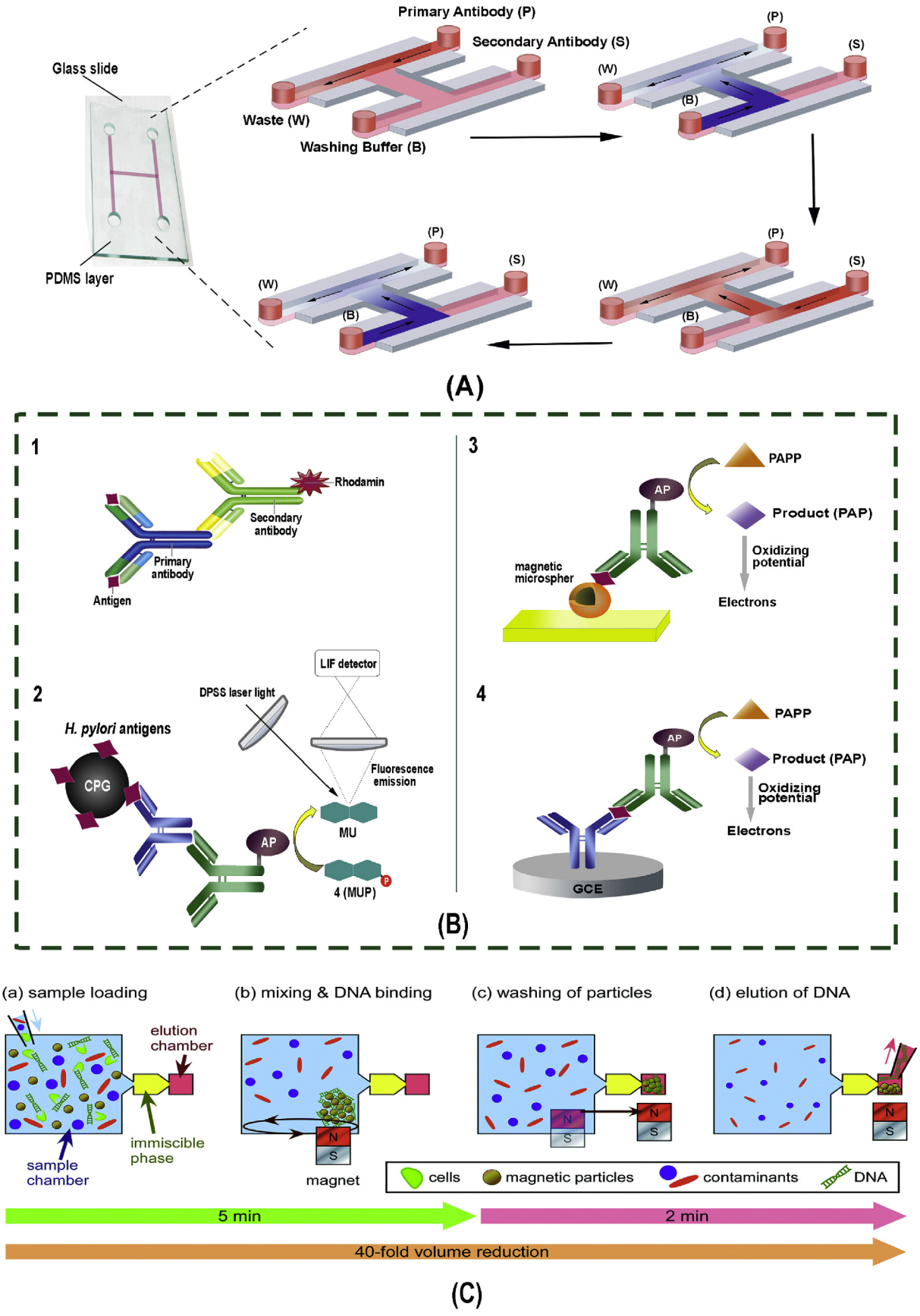

Fig. 6. Nano/microfluidic technologies for detection of *H. pylori* infection. (A) Schematic of an immunoassay chip with an H-shaped microchannel for the detection of *H. pylori*-specific IgG antibodies; reproduced from published paper [106]. (B) Some of immunoreaction at microchannels of microfluidic [105,107,108,110]. (C) Schematic drawing of the setup for the *H. pylori* DNA extraction process; reprinted with permission from Ref. [6].

between antibodies in serum samples and the immobilized antigens were determined using alkaline phosphatase (AP) enzyme-labeled second antibodies specific to human IgG. In a study employing AP enzyme-labeled second antibody properties coupled with laser-induced fluorescent (LIF) detection system, a high sensitivity portable microfluidic immunosensor was realized [107]. In this platform, 4-methylumbelliferyl phosphate (4-MUP) employed as an enzymatic substrate, was converted to soluble fluorescent methylumbelliferone by AP. The device had a central channel (CC) with packed *H. pylori* antigen immobilized on APCPG. Antibodies in serum samples reacted immunologically with the immobilized antigen and then, the bound antibodies were quantified by AP enzyme-labeled second antibodies specific to human IgG. The fluorescent product was finally quantified by LIF detection (Fig. 6-B2). The calculated detection limits for LIF detection and the ELISA procedure were 0.17 mL $^{-1}$ and 2.1 U mL^{-1}, respectively, and the assay coefficients of variation were below 5.1% [107].

In another study, Molina et al. [108] reported a bioanalytical platform based on the multiple use of an immobilized *H. pylori* antigen on an immuno-column incorporated into a flow-injection (FI) analytical system. Heterogeneous enzyme immunoassays, assembled with the FI system and electrochemical detection, demonstrated a potent analytical tool for the determination of low amount of many analytes including hormones, tumor markers, drugs, antibodies, and microorganism [109]. They employed the immuno-adsorbent column, which packed by 3-aminopropyl-modified controlled-pore glass (APCPG) covalently linking *H. pylori* antigens in Teflon tubing. *p*-Aminophenyl phosphate (*p*APP) was converted to *p*-aminophenol (*p*AP) by AP, and an electroactive product was quantified on glassy carbon electrode (GCE) modified with multi-wall carbon nanotubes (MWCNT) at 0.30 V (Fig. 6-B3). This method allowed for a rapid determination of target in about 25 min. The LOD for amperometric detection and the ELISA procedure was obtained 0.62 $^{-1}$ and 1.8 U mL^{-1}, respectively [108]. In a similar manner, Pereira et al. (2010) developed a microfluidic enzyme-linked-immunomagnetic assay coupled to a gold electrode using a non-competitive immunoassay. In this system, purified *H. pylori* antigens, immobilized on magnetic microspheres, and were injected into the microchannel of the device. The electroactive product resulted from AP reaction (conversion of *p*APP to *p*Ap) was detected on gold coated electrode at 0.250 V (Fig. 6-B4). The electrochemical detection could be performed within 1 min and the overall assay time was 25 min. This study demonstrated a LOD of 0.37 UmL^{-1} in terms of electrochemical detection and 2.1 UmL^{-1} for the ELISA procedure [110].

Recently, some *H. pylori* strains have evolved to be resistant to generally used antibiotics such as quinolones. Quinolones target bacterial DNA gyrase. Recently, two DNA point mutations on the gyrase A subunit lead to quinolone-resistance in *H. pylori* [111]. Therefore, the detection of these two single-point mutations is of major demand for *H. pylori* treatment. Based on this idea, Chao et al. [112] established an advanced diagnostic assay carrying out an incorporated microfluidic system for quick detection of antibiotic resistance in *H. pylori*. The device integrates several microfluidic components including micropumps, normally-closed microvalves, and reaction chambers. The on-chip diagnostic process was performed in three steps: (i) nucleic acid extraction by specific probe-conjugated magnetic beads, (ii) amplification of the target DNA fragments including those indicative of resistance to quinolone antibiotics by using on-chip PCR and on-chip SNP-PCR, and (iii) an optical detection which was able to precisely detect the fluorescence signals generated by intercalating of SYBRs Green I to the PCR amplicons. In this study, the detection limit was 10^2 bacterial cells for *H. pylori* detection and two different SNP sites in strains. Furthermore, the entire process could be performed within only 60 min without human intervention [112].

Finally, Mosley et al. reported a sample introduction junction that allowed direct on-chip processing of crude stool samples for the detection of *H. pylori*. In this study, DNA extraction was performed by IFAST (immiscible filtration assisted by surface tension) in large volume sample chamber with a septum-based interface for stool sample introduction. Then, superparamagnetic particles

Table 3
Comparison of advantages and limitations of various methods for *H. pylori* detection.

Principle	Advantages	Limitations	Ref.
Conventional methods[a]	- Widely available - Considered as routine diagnostic method	- Time-consuming - Mostly requires specific and expensive equipment - Utilize high quantity of costly reagents - Varying precision and sensitivity in diverse clinical conditions and settings	[4,23,32]
Optical biosensor	- Quantitative, - Free of amplification, labeling and advanced instruments - Mostly readable with the naked eye in colorimetric assay	- Commonly costly with low portability (for fluorescence based biosensors) - Has not been used in clinic - Fabrication of biosensor requires is time consuming	[42,47]
Electrochemical biosensor	- Quantitative - Reusability - Low amount of sample/reagent volumes are required	- Has not been used in clinic - Limited control on the working electrode surface with higher currents - False positive results due to electrolytes from the samples	[42,76,77]
Paper-based (Lateral flow tests)	- Simple, efficient, affordable, easy to use and rapid - Stable performance over a varied range of time and temperature - No need to pure sample and additional reagents - Commercially available for applicability in lab - Not require complicated equipment - Mostly readable with the naked eye	- Paper can be disposed or burned easily - The difficulty in the implementation of fluidic manipulation on paper strips - Require careful attentions for precise liquid handling and distribution - The difficulty in performing multiplex and quantitative analyses High limit of detection	[37,90,91,93]
Microfluidic (Lab-on-a-chip)	- High throughput analysis, miniaturization and automation - ASSURED (affordable, sensitive, specific, user friendly, rapid and robust, equipment-free, and deliverable to end-users technologies) - Low consumption of samples and reagents as well reaction and assay time	- Has not been employed in clinic - Technical expertise is necessary for operating complex machinery - The limited lifespan of microfluidic chips due to blocking or clogging	[37,38,98]

[a] These methods classified into invasive and noninvasive tests. For detailed comparison of advantages and disadvantages of each test refer to [23].

(PMPs) mixed with sample and released DNA from *H. pylori* cells binded to the PMPs. Finally, the PMPs were transferred via a magnet through the immiscible oil phase into an elution chamber where the DNA was released into aqueous media for subsequent assays. The entire process required only 7 min while enabling a 40-fold reduction in working volume from crude biological samples (Fig. 6C) [6]. This miniaturized approach offers high potential for commercially stool DNA extraction kits.

4. Conclusions and future perspectives

This review presented an overview on recent advances in the development of nanomaterial-based biosensors and microfluidic systems for *H. pylori* detection. *H. pylori* is recognized as initial cause of various gastrointestinal diseases. Thus, its proper diagnosis is of high importance. Rapid diagnosis and treatment of infection in its early stages play a major role in inhibiting the spread of *H. pylori* infection. To this end, many methods have been developed as rapid and point-of-care diagnostics for *H. pylori* infections. The major challenge in designing detection methods and tools is mainly revolving around identifying biomarkers that are credible and reliable for *H. pylori* detection. For the emerging diagnostic methods, it is expected that either new biomarkers or existing biomarkers with desirable characteristics will be employed. Combination of potential recombinant forms of antigenic proteins with nanomaterial-based biosensing has created new opportunities for diagnosis of *H. pylori* infections.

Despite the advantages of nanomaterials, the present state of nanomaterial-based biosensors showed some limitations such as functional moieties in a number of the nanomaterials and the difficulty in bioconjugation chemistry. To overcome such obstacles, immunoassays for the diagnosis of *H. pylori* could be realized using nano/microfluidic platforms with integrated nanomaterials. Such on-chip sensing devices can provide high sensitivity and mitigate background noise signals. Comparison of advantages and limitations of conventional biosensing and new advanced miniaturized diagnostic methods are summarized in Table 3.

Aptamers are considered as favorite candidates for designing on-chip sensors due to their capability in conducting rapid, easy, and sensitive detection of targeted molecules. The three-dimensional and stable architecture of aptamers enable very high sensitivity detections compared to antibody-based sensors. Microfluidic-based aptasensors can be designed for automated operation where all steps of an immunoassay are performed in a programmed manner to remove human errors and improve accuracy. Such on-chip systems can be further miniaturized by integration with smartphones and flexible electronics for signal readout and display purposes.

Acknowledgments

Funding for the laboratories of MR and KA has been received from Mashhad University of Medical Sciences (MUMS), Mashhad, Iran. SAMS acknowledges financial support from Iran's National Elites Foundation and Iran Nanotechnology Initiative Council (INIC) to support writing this article.

References

[1] N.R. Salama, M.L. Hartung, A. Muller, Life in the human stomach: persistence strategies of the bacterial pathogen *Helicobacter pylori*, Nat. Rev. Microbiol. 11 (2013) 385–399.
[2] M. Amieva, R.M. Peek, Pathobiology of *Helicobacter pylori*–induced gastric cancer, Gastroenterology 150 (2016) 64–78.
[3] J.G. Kusters, A.H. van Vliet, E.J. Kuipers, Pathogenesis of *Helicobacter pylori* infection, Clin. Microbiol. Rev. 19 (2006) 449–490.
[4] P. Malfertheiner, A. Link, M. Selgrad, *Helicobacter pylori*: perspectives and time trends, Nat. Rev. Gastroenterol. Hepatol. 11 (2014) 628–638.
[5] N. Uemura, S. Okamoto, S. Yamamoto, N. Matsumura, S. Yamaguchi, M. Yamakido, K. Taniyama, N. Sasaki, R.J. Schlemper, *Helicobacter pylori* infection and the development of gastric cancer, N. Engl. J. Med. 345 (2001) 784–789.
[6] O. Mosley, L. Melling, M. Tarn, C. Kemp, M. Esfahani, N. Pamme, K. Shaw, Sample introduction interface for on-chip nucleic acid-based analysis of *Helicobacter pylori* from stool samples, Lab Chip 16 (2016) 2108–2115.
[7] H. Nordenstedt, D.Y. Graham, J.R. Kramer, M. Rugge, G. Verstovsek, S. Fitzgerald, A. Alsarraj, Y. Shaib, M.E. Velez, N. Abraham, *Helicobacter pylori*-negative gastritis: prevalence and risk factors, Am. J. Gastroenterol. 108 (2013) 65–71.
[8] A. Zullo, C. Hassan, F. Cristofari, A. Andriani, V. De Francesco, E. Ierardi, S. Tomao, M. Stolte, S. Morini, D. Vaira, Effects of *Helicobacter pylori* eradication on early stage gastric mucosa–associated lymphoid tissue lymphoma, Clin. Gastroenterol. Hepatol. 8 (2010) 105–110.
[9] S.Y. Ly, H.-S. Yoo, S.H. Choa, Diagnosis of *Helicobacter pylori* bacterial infections using a voltammetric biosensor, J. Microbiol. Methods 87 (2011) 44–48.
[10] M.R. Amieva, E.M. El-Omar, Host-bacterial interactions in *Helicobacter pylori* infection, Gastroenterology 134 (2008) 306–323.
[11] Y. Yamaoka, Mechanisms of disease: *Helicobacter pylori* virulence factors, Nat. Rev. Gastroenterol. Hepatol. 7 (2010) 629–641.
[12] M. Bernard, C. Josenhans, Pathogenesis of *Helicobacter pylori* infection, Helicobacter 19 (2014) 11–18.
[13] R.M. Delahay, M. Rugge, Pathogenesis of *Helicobacter pylori* infection, Helicobacter 17 (2012) 9–15.
[14] B.M. Roesler, E.M. Rabelo-Gonçalves, J.M. Zeitune, Virulence factors of *Helicobacter pylori*: a review, Clin. Med. Insights Gastroenterol. 7 (2014) 9.
[15] A. Khalilpour, M. Kazemzadeh-Narbat, A. Tamayol, R. Oklu, A. Khademhosseini, Biomarkers and diagnostic tools for detection of *Helicobacter pylori*, Appl. Microbiol. Biotechnol. 100 (2016) 4723–4734.
[16] C.-Y. Kao, B.-S. Sheu, J.-J. Wu, *Helicobacter pylori* infection: an overview of bacterial virulence factors and pathogenesis, Biomed. J. 39 (2016) 14–23.
[17] M. Hatakeyama, Oncogenic mechanisms of the *Helicobacter pylori* CagA protein, Nat. Rev. Cancer 4 (2004) 688–694.
[18] T.L. Cover, S.R. Blanke, *Helicobacter pylori* VacA, a paradigm for toxin multifunctionality, Nat. Rev. Microbiol. 3 (2005) 320–332.
[19] S.L. Palframan, T. Kwok, K. Gabriel, Vacuolating cytotoxin A (VacA), a key toxin for *Helicobacter pylori* pathogenesis, Front. Cell Infect. Microbiol. 2 (2012) 92.
[20] T.P. Cid, M.C. Fernández, S. Benito Martínez, N.L. Jones, Pathogenesis of *Helicobacter pylori* infection, Helicobacter 18 (2013) 12–17.
[21] D.B. Polk, R.M. Peek, *Helicobacter pylori*: gastric cancer and beyond, Nat. Rev. Cancer 10 (2010) 403–414.
[22] M. Junaid, A.K. Linn, M.B. Javadi, S. Al-Gubare, N. Ali, G. Katzenmeier, Vacuolating cytotoxin A (VacA) – a multi-talented pore-forming toxin from *Helicobacter pylori*, Toxicon 118 (2016) 27–35.
[23] N.S. Atkinson, B. Braden, *Helicobacter pylori* infection: diagnostic strategies in primary diagnosis and after therapy, Dig. Dis. Sci. 61 (2016) 19–24.
[24] E. Garza-González, G.I. Perez-Perez, H.J. Maldonado-Garza, F.J. Bosques-Padilla, A review of *Helicobacter pylori* diagnosis, treatment, and methods to detect eradication, World J. Gastroenterol. 20 (2014) 1438–1449.
[25] P. Malfertheiner, Diagnostic methods for *H. pylori* infection: choices, opportunities and pitfalls, United Eur. Gastroenterol. J. 3 (2015) 429–431.
[26] M. Douraghi, M.N. Rostami, H. Goudarzi, Z. Ghalavand, Comparison of stool antigen immunoassay and serology for screening for *Helicobacter pylori* infection in intellectually disabled children, Microbiol. Immunol. 57 (2013) 772–777.
[27] B.-L. Yang, C. Yeh, W.-G. Kwong, S.-D. Lee, A novel one-step *Helicobacter pylori* saliva antigen test, J. Chin. Med. Assoc. 78 (2015) 96–100.
[28] S. Koletzko, Noninvasive diagnostic tests for *Helicobacter pylori* infection in children, Can. J. Gastroenterol. Hepatol. 19 (2005) 433–439.
[29] J. Gisbert, J. Pajares, Review article: ^{13}C-urea breath test in the diagnosis of *Helicobacter pylori* infection–a critical review, Aliment. Pharmacol. Ther. 20 (2004) 1001–1017.
[30] K.S. Gurusamy, M. Yaghoobi, B.R. Davidson, Non-invasive diagnostic tests for *Helicobacter pylori* infection, Cochrane Libr. (2016), CD012080.
[31] M. El Khadir, S.A. Boukhris, D.-A. Benajah, K. El Rhazi, S.A. Ibrahimi, M. El Abkari, T. Harmouch, C. Nejjari, M. Mahmoud, M. Benlemlih, Detection of *Helicobacter pylori* urease antigen in saliva in patients with different gastric *H. pylori* status, J. Chin. Med. Assoc. 79 (2016) 363–367.
[32] B. Kalali, L. Formichella, M. Gerhard, Diagnosis of *Helicobacter pylori*: changes towards the future, Diseases 3 (2015) 122–135.
[33] A. Bhattacharyya, C. Klapperich, Design and testing of a disposable microfluidic chemiluminescent immunoassay for disease biomarkers in human serum samples, Biomed. Microdevices 9 (2007) 245–251.
[34] S. Choi, M. Goryll, L.Y.M. Sin, P.K. Wong, J. Chae, Microfluidic-based biosensors toward point-of-care detection of nucleic acids and proteins, Microfluid Nanofluidics 10 (2011) 231–247.
[35] H. Ozkan, O.S. Kayhan, A novel automatic rapid diagnostic test reader platform, Comput. Math. Methods Med. 2016 (2016).
[36] J. Ezzati Nazhad Dolatabadi, M. de la Guardia, Nanomaterial-based electrochemical immunosensors as advanced diagnostic tools, Anal. Methods 6 (2014) 3891–3900.

[37] J. Hu, S. Wang, L. Wang, F. Li, B. Pingguan-Murphy, T.J. Lu, F. Xu, Advances in paper-based point-of-care diagnostics, Biosens. Bioelectron. 54 (2014) 585–597.
[38] W. Su, X. Gao, L. Jiang, J. Qin, Microfluidic platform towards point-of-care diagnostics in infectious diseases, J. Chromatogr. A 1377 (2015) 13–26.
[39] N.-T. Nguyen, S.A.M. Shaegh, N. Kashaninejad, D.-T. Phan, Design, fabrication and characterization of drug delivery systems based on lab-on-a-chip technology, Adv. Drug Deliv. Rev. 65 (2013) 1403–1419.
[40] A. Mokhtarzadeh, J.E.N. Dolatabadi, K. Abnous, M. de la Guardia, M. Ramezani, Nanomaterial-based cocaine aptasensors, Biosens. Bioelectron. 68 (2015) 95–106.
[41] R.Y. Robati, A. Arab, M. Ramezani, F.A. Langroodi, K. Abnous, S.M. Taghdisi, Aptasensors for quantitative detection of kanamycin, Biosens. Bioelectron. 82 (2016) 162–172.
[42] A.A. Jamali, M. Pourhassan-Moghaddam, J.E.N. Dolatabadi, Y. Omidi, Nanomaterials on the road to microRNA detection with optical and electrochemical nanobiosensors, Trends Anal. Chem. TrAC 55 (2014) 24–42.
[43] J. Raba, M.A. Fernández-Baldo, S.V. Pereira, G.A. Messina, F.A. Bertolino, S. Tosetti, M.I.S. Ferramola, Analytical biosensors for the pathogenic microorganisms determination, 2013.
[44] A. de la Escosura-Muñiz, C. Parolo, A. Merkoçi, Immunosensing using nanoparticles, Mater. Today 13 (2010) 24–34.
[45] N.J. Ronkainen, S.L. Okon, Nanomaterial-based electrochemical immunosensors for clinically significant biomarkers, Materials 7 (2014) 4669–4709.
[46] H.F. Cui, T.-B. Xu, Y.-L. Sun, A.-W. Zhou, Y.-H. Cui, W. Liu, J.H. Luong, Hairpin DNA as a biobarcode modified on gold nanoparticles for electrochemical DNA detection, Anal. Chem. 87 (2015) 1358–1365.
[47] V. Perumal, U. Hashim, Advances in biosensors: principle, architecture and applications, J. Appl. Biomed. 12 (2014) 1–15.
[48] A. Nezami, R. Nosrati, B. Golichenari, R. Rezaee, G.I. Chatzidakis, A.M. Tsatsakis, G. Karimi, Nanomaterial-based aptasensors and bioaffinity sensors for quantitative detection of 17β-estradiol, TrAC Trends Anal. Chem. 94 (2017) 95–105.
[49] C. Feng, S. Dai, L. Wang, Optical aptasensors for quantitative detection of small biomolecules: a review, Biosens. Bioelectron. 59 (2014) 64–74.
[50] G. Wang, Y. Wang, L. Chen, J. Choo, Nanomaterial-assisted aptamers for optical sensing, Biosens. Bioelectron. 25 (2010) 1859–1868.
[51] F. Teles, L. Fonseca, Trends in DNA biosensors, Talanta 77 (2008) 606–623.
[52] M. Shahdordizadeh, S.M. Taghdisi, N. Ansari, F. Alebooye Langroodi, K. Abnous, M. Ramezani, Aptamer based biosensors for detection of *Staphylococcus aureus*, Sensors Actuators B Chem. 241 (2017) 619–635.
[53] M. Shanehsaz, A. Mohsenifar, S. Hasannia, N. Pirooznia, Y. Samaei, M. Shamsipur, Detection of *Helicobacter pylori* with a nanobiosensor based on fluorescence resonance energy transfer using CdTe quantum dots, Microchim. Acta 180 (2013) 195–202.
[54] J. Shi, F. Tian, J. Lyu, M. Yang, Nanoparticle based fluorescence resonance energy transfer (FRET) for biosensing applications, J. Mater. Chem. B 3 (2015) 6989–7005.
[55] F. Charbgoo, F. Soltani, S.M. Taghdisi, K. Abnous, M. Ramezani, Nanoparticles application in high sensitive aptasensor design, TrAC Trends Anal. Chem. 85, Part C (2016) 85–97.
[56] J.E.N. Dolatabadi, O. Mashinchian, B. Ayoubi, A.A. Jamali, A. Mobed, D. Losic, Y. Omidi, M. de la Guardia, Optical and electrochemical DNA nanobiosensors, Trends Anal. Chem. TrAC 30 (2011) 459–472.
[57] U. Alexiev, P. Volz, A. Boreham, R. Brodwolf, Time-resolved fluorescence microscopy (FLIM) as an analytical tool in skin nanomedicine, Eur. J. Pharm. Biopharm. 116 (2017) 111–124.
[58] Z. Liu, X. Su, A novel fluorescent DNA sensor for ultrasensitive detection of *Helicobacter pylori*, Biosens. Bioelectron. 87 (2017) 66–72.
[59] R. Freeman, I. Willner, Optical molecular sensing with semiconductor quantum dots (QDs), Chem. Soc. Rev. 41 (2012) 4067–4085.
[60] S. Jin, Y. Hu, Z. Gu, L. Liu, H.-C. Wu, Application of quantum dots in biological imaging, J. Nanomater. 2011 (2011) 13.
[61] M.S. Mannoor, H. Tao, J.D. Clayton, A. Sengupta, D.L. Kaplan, R.R. Naik, N. Verma, F.G. Omenetto, M.C. McAlpine, Graphene-based wireless bacteria detection on tooth enamel, Nat. Commun. 3 (2012) 763.
[62] C. Chung, Y.-K. Kim, D. Shin, S.-R. Ryoo, B.H. Hong, D.-H. Min, Biomedical applications of graphene and graphene oxide, Accounts Chem. Res. 46 (2013) 2211–2224.
[63] S.K. Ghosh, T. Pal, Interparticle coupling effect on the surface plasmon resonance of gold nanoparticles: from theory to applications, Chem. Rev. 107 (2007) 4797–4862.
[64] M. Rex, F.E. Hernandez, A.D. Campiglia, Pushing the limits of mercury sensors with gold nanorods, Anal. Chem. 78 (2006) 445–451.
[65] M. Shahrashoob, A. Mohsenifar, M. Tabatabaei, T. Rahmani-Cherati, M. Mobaraki, A. Mota, T. Shojaei, Detection of *Helicobacter pylori* genome with an optical biosensor based on hybridization of urease gene with a gold nanoparticles-labeled probe, J. Appl. Spectrosc. 83 (2016) 322–329.
[66] E.C. Dreaden, A.M. Alkilany, X. Huang, C.J. Murphy, M.A. El-Sayed, The golden age: gold nanoparticles for biomedicine, Chem. Soc. Rev. 41 (2012) 2740–2779.
[67] P. Gill, M. Amini, A. Ghaemi, L. Shokouhizadeh, H. Abdul-Tehrani, A. Karami, A. Gilak, Detection of *Helicobacter pylori* by enzyme-linked immunosorbent assay of thermophilic helicase-dependent isothermal DNA amplification, Diagn. Microbiol. Infect. Dis. 59 (2007) 243–249.
[68] P. Gill, A.-H. Alvandi, H. Abdul-Tehrani, M. Sadeghizadeh, Colorimetric detection of *Helicobacter pylori* DNA using isothermal helicase-dependent amplification and gold nanoparticle probes, Diagn. Microbiol. Infect. Dis. 62 (2008) 119–124.
[69] H. Wang, X. Wang, J. Wang, W. Fu, C. Yao, A SPR biosensor based on signal amplification using antibody-QD conjugates for quantitative determination of multiple tumor markers, Sci. Rep. 6 (2016) 33140.
[70] O. Lazcka, F.J. Del Campo, F.X. Munoz, Pathogen detection: a perspective of traditional methods and biosensors, Biosens. Bioelectron. 22 (2007) 1205–1217.
[71] T. Nishimura, E. Hifumi, T. Fujii, Y. Niimi, N. Egashira, K. Shimizu, T. Uda, Measurement of *Helicobacter pylori* using anti its urease monoclonal antibody by surface plasmon resonance, Electrochemistry 68 (2000) 916–919.
[72] M. Utt, B. Danielsson, T. Wadström, *Helicobacter pylori* vacuolating cytotoxin binding to a putative cell surface receptor, heparan sulfate, studied by surface plasmon resonance, FEMS Immunol. Med. Microbiol. 30 (2001) 109–113.
[73] E. Fabini, B. Zambelli, L. Mazzei, S. Ciurli, C. Bertucci, Surface plasmon resonance and isothermal titration calorimetry to monitor the Ni(II)-dependent binding of *Helicobacter pylori* NikR to DNA, Anal. Bioanal. Chem. 408 (2016) 7971–7980.
[74] J. Homola, Present and future of surface plasmon resonance biosensors, Anal. Bioanal. Chem. 377 (2003) 528–539.
[75] X. Su, S.F.Y. Li, Serological determination of *Helicobacter pylori* infection using sandwiched and enzymatically amplified piezoelectric biosensor, Anal. Chim. Acta 429 (2001) 27–36.
[76] A.A. Saei, J.E.N. Dolatabadi, P. Najafi-Marandi, A. Abhari, M. de la Guardia, Electrochemical biosensors for glucose based on metal nanoparticles, Trends Anal. Chem. TrAC 42 (2013) 216–227.
[77] X. Zuo, S. Song, J. Zhang, D. Pan, L. Wang, C. Fan, A target-responsive electrochemical aptamer switch (TREAS) for reagentless detection of nanomolar ATP, J. Am. Chem. Soc. 129 (2007) 1042–1043.
[78] Y.-n. He, H.-y. Chen, J.-j. Zheng, G.-y. Zhang, Z.-L. Chen, Differential pulse voltammetric enzyme-linked immunoassay for the determination of *Helicobacter pylori* specific immunoglobulin G (IgG) antibody, Talanta 44 (1997) 823–830.
[79] M. Del Pozo, C. Alonso, F. Pariente, E. Lorenzo, DNA biosensor for detection of *Helicobacter pylori* using phen-dione as the electrochemically active ligand in osmium complexes, Anal. Chem. 77 (2005) 2550–2557.
[80] M. Revenga-Parra, T. García, E. Lorenzo, F. Pariente, Comprehensive study of interactions between DNA and new electroactive Schiff base ligands: application to the detection of singly mismatched *Helicobacter pylori* sequences, Biosens. Bioelectron. 22 (2007) 2675–2681.
[81] S.K. Vashist, D. Zheng, K. Al-Rubeaan, J.H. Luong, F.-S. Sheu, Advances in carbon nanotube based electrochemical sensors for bioanalytical applications, Biotechnol. Adv. 29 (2011) 169–188.
[82] S. Taghavi, S. Ayatollahi, M. Alibolandi, P. Lavaee, M. Ramezani, K. Abnous, A novel label-free cocaine assay based on aptamer-wrapped single-walled carbon nanotubes, Nanomed. J. 1 (2014) 100–106.
[83] T. García, M. Revenga-Parra, H. Abruna, F. Pariente, E. Lorenzo, Single-mismatch position-sensitive detection of DNA based on a bifunctional ruthenium complex, Anal. Chem. 80 (2008) 77–84.
[84] T. García, E. Casero, M. Revenga-Parra, J. Martín-Benito, F. Pariente, L. Vázquez, E. Lorenzo, Architectures based on the use of gold nanoparticles and ruthenium complexes as a new route to improve genosensor sensitivity, Biosens. Bioelectron. 24 (2008) 184–190.
[85] C. Sun, L. Zhang, J. Jiang, G. Shen, R. Yu, Electrochemical DNA biosensor based on proximity-dependent DNA ligation assays with DNAzyme amplification of hairpin substrate signal, Biosens. Bioelectron. 25 (2010) 2483–2489.
[86] I. Willner, B. Shlyahovsky, M. Zayats, B. Willner, DNAzymes for sensing, nanobiotechnology and logic gate applications, Chem. Soc. Rev. 37 (2008) 1153–1165.
[87] B. Dindar, E. Karakuş, F. Abasıyanık, New urea biosensor based on urease enzyme obtained from *Helycobacter pylori*, Appl. Biochem. Biotechnol. 165 (2011) 1308–1321.
[88] N. Nasirizadeh, M.S. Hejazi, P. Yaghmai, An electrochemical DNA biosensor based on Oracet Blue as a label for detection of *Helicobacter pylori*, Int. J. Biol. Macromol. (2016).
[89] S. Hajihosseini, N. Nasirizadeh, M.S. Hejazi, P. Yaghmaei, A sensitive DNA biosensor fabricated from gold nanoparticles and graphene oxide on a glassy carbon electrode, Mater. Sci. Eng. C 61 (2016) 506–515.
[90] C. Parolo, A. Merkoçi, Paper-based nanobiosensors for diagnostics, Chem. Soc. Rev. 42 (2013) 450–457.
[91] E.B. Bahadır, M.K. Sezgintürk, Lateral flow assays: principles, designs and labels, TrAC Trends Anal. Chem. 82 (2016) 286–306.
[92] M.J. Raeisossadati, N.M. Danesh, F. Borna, M. Gholamzad, M. Ramezani, K. Abnous, S.M. Taghdisi, Lateral flow based immunobiosensors for detection of food contaminants, Biosens. Bioelectron. 86 (2016) 235–246.
[93] X. Ge, A.M. Asiri, D. Du, W. Wen, S. Wang, Y. Lin, Nanomaterial-enhanced paper-based biosensors, Trends Anal. Chem. Trac. 58 (2014) 31–39.
[94] C. Karakus, B.A. Salih, Comparison of the lateral flow immunoassays (LFIA) for the diagnosis of *Helicobacter pylori* infection, J. Immunol. method 396 (2013) 8–14.
[95] K.R. Hawkins, B.H. Weigl, Microfluidic diagnostics for low-resource settings, in: MOEMS-MEMS, International Society for Optics and Photonics, 2010, 75930L-75930L-75915.

[96] G.M. Whitesides, The origins and the future of microfluidics, Nature 442 (2006) 368–373.
[97] D.-T. Phan, S.A.M. Shaegh, C. Yang, N.-T. Nguyen, Sample concentration in a microfluidic paper-based analytical device using ion concentration polarization, Sensors Actuators B Chem. 222 (2016) 735–740.
[98] R. Riahi, A. Tamayol, S.A.M. Shaegh, A.M. Ghaemmaghami, M.R. Dokmeci, A. Khademhosseini, Microfluidics for advanced drug delivery systems, Curr. Opin. Chem. Eng. 7 (2015) 101–112.
[99] T. Laksanasopin, C.D. Chin, H. Moore, J. Wang, Y.K. Cheung, S.K. Sia, Microfluidic point-of-care diagnostics for resource-poor environments, in: SPIE Defense, Security, and Sensing, International Society for Optics and Photonics, 2009, 73180E-73180E-73186.
[100] F. Cui, M. Rhee, A. Singh, A. Tripathi, Microfluidic sample preparation for medical diagnostics, Annu. Rev. Biomed. Eng. 17 (2015) 267–286.
[101] B. Giri, B. Pandey, B. Neupane, F.S. Ligler, Signal amplification strategies for microfluidic immunoassays, TrAC Trends Anal. Chem. 79 (2016) 326–334.
[102] R. Riahi, S.A.M. Shaegh, M. Ghaderi, Y.S. Zhang, S.R. Shin, J. Aleman, S. Massa, D. Kim, M.R. Dokmeci, A. Khademhosseini, Automated microfluidic platform of bead-based electrochemical immunosensor integrated with bioreactor for continual monitoring of cell secreted biomarkers, Sci. Rep. 6 (2016) 24598.
[103] F.Y. Lin, M. Sabri, D. Erickson, J. Alirezaie, D. Li, P.M. Sherman, Development of a novel microfluidic immunoassay for the detection of *Helicobacter pylori* infection, Analyst 129 (2004) 823–828.
[104] F.Y. Lin, M. Sabri, J. Alirezaie, D. Li, P.M. Sherman, Development of a nanoparticle-labeled microfluidic immunoassay for detection of pathogenic microorganisms, Clin. Diagn. Lab. Immunol. 12 (2005) 418–425.
[105] Y. Gao, F.Y. Lin, G. Hu, P.M. Sherman, D. Li, Development of a novel electrokinetically driven microfluidic immunoassay for the detection of *Helicobacter pylori*, Anal. Chim. Acta 543 (2005) 109–116.
[106] Y. Gao, G. Hu, F.Y. Lin, P.M. Sherman, D. Li, Development of an automatic electrokinetically-controlled microfluidic immunoassay for the detection of *Helicobacter pylori*, in: ASME 3rd International Conference on Microchannels and Minichannels, American Society of Mechanical Engineers, 2005, pp. 495–502.
[107] M.A. Seia, S.V. Pereira, C.A. Fontán, I.E. De Vito, G.A. Messina, J. Raba, Laser-induced fluorescence integrated in a microfluidic immunosensor for quantification of human serum IgG antibodies to *Helicobacter pylori*, Sens. Actuator B Chem. 168 (2012) 297–302.
[108] L. Molina, G.A. Messina, P.W. Stege, E. Salinas, J. Raba, Immuno-column for on-line quantification of human serum IgG antibodies to *Helicobacter pylori* in human serum samples, Talanta 76 (2008) 1077–1082.
[109] C.A. Marquette, L.J. Blum, State of the art and recent advances in immunoanalytical systems, Biosens. Bioelectron. 21 (2006) 1424–1433.
[110] S.V. Pereira, G.A. Messina, J. Raba, Integrated microfluidic magnetic immunosensor for quantification of human serum IgG antibodies to *Helicobacter pylori*, J. Chromatogr. B 878 (2010) 253–257.
[111] K.H. Hung, B.S. Sheu, W.L. Chang, H.M. Wu, C.C. Liu, J.J. Wu, Prevalence of primary fluoroquinolone resistance among clinical isolates of *Helicobacter pylori* at a University Hospital in Southern Taiwan, Helicobacter 14 (2009) 61–65.
[112] C.-Y. Chao, C.-H. Wang, Y.-J. Che, C.-Y. Kao, J.-J. Wu, G.-B. Lee, An integrated microfluidic system for diagnosis of the resistance of *Helicobacter pylori* to quinolone-based antibiotics, Biosens. Bioelectron. 78 (2016) 281–289.